8-2021

RECONSTRUCTING 1856-7 CALIFORNIA MINING PATTERNS FROM PLACER GOLD RECOVERED FROM THE WRECK OF THE SS CENTRAL AMERICA

Kathryn Ruth VonSydow
California State University - San Bernardino

RECONSTRUCTING 1856-7 CALIFORNIA MINING PATTERNS FROM PLACER GOLD RECOVERED FROM THE WRECK OF THE SS CENTRAL AMERICA

A Thesis

Presented to the

Faculty of

California State University,

San Bernardino

In Partial Fulfillment

of the Requirements for the Degree

Master of Science

in

Earth and Environmental Sciences:

Geology

---

by

Kathryn Ruth VonSydow

August 2021

RECONSTRUCTING 1856-7 CALIFORNIA MINING PATTERNS FROM PLACER GOLD RECOVERED FROM THE WRECK OF THE SS CENTRAL AMERICA

A Thesis

Presented to the

Faculty of

California State University,

San Bernardino

---

by

Kathryn Ruth VonSydow

August 2021

Approved by:

Dr. Erik Melchiorre, Committee Chair, Geology

Dr. Codi Lazar, Committee Member

Dr. Britt Leatham, Committee Member

ABSTRACT

The discovery of the SS Central America 1857 shipwreck site provides a time capsule that can be used to address questions about the spatial and temporal patterns of placer mining in California during the peak of the gold rush. Samples of placer gold in the collections of museums and private individuals can have uncertain pedigree due to labeling issues and alterations by cleaning and curatorial processes. However, placer gold from the 1857 shipwreck could only have come from the Mother Lode Country of California, as no other gold districts had yet been found in western North America. I compared the chemistry and mineralogy of well-characterized mid-19th century Mother Lode placer gold to the properties of the placer gold recovered within a safe from the shipwreck, which contained a vest with four pokes sewn into pockets. My analysis of gold from three of the pokes indicates that each was collected from a different area. Poke 1 has crystalline gold fragments that were found close to a gold source and rounded pieces that originated farther upstream. Platinum-group metal grains indicate this gold was sourced from the Yuba River. Poke 2 gold has inclusions of anglesite, a common secondary lead mineral that forms from the oxidation of galena. Anglesite inclusions in gold are rare in the Sierras, only found along the Feather River. Gold from Poke 3 has many inclusions of quartz and feldspar, which suggest close proximity to a lode gold source.

The ubiquitous traces of mercury (Hg) on the surface of the gold suggests that all the placer gold came from sites of significant mining operations as

established mines used mercury at the time. The shape, geochemistry, and context of the placer gold imply that this gold was collected from active mining centers along the upper Yuba and upper Feather Rivers. Morphology and chemistry of the gold indicate all was collected within 15 km of the bedrock lode sources. Furthermore, almost all other gold on the shipwreck was found in passenger rooms and cargo areas. Gold from this study was found in the ship pursers' safe in secret compartments in a vest, implying an owner with connections and discretion beyond those of a simple miner. Given this evidence, it is suggested that the placer gold was collected at several major mining camps by a professional gold buyer or mining engineer.

ACKNOWLEDGEMENTS

This was among one of the hardest tasks I have undertaken to date and would have failed miserably without the love and support of my family, friends, and academic advisors. I would like to recognize some people that helped make this thesis possible.

First and foremost, I have to thank the person that has always been my biggest supporter and my best friend, my mother, Donna Hendrickson. I love you with all of my heart, Mom. Thank you for always inspiring me to keep going.

Secondly, I have to thank my bestie, Renee Williams. I love you so much and am so thankful to have you in my life. Thank you for always being my cheerleader and keeping me motivated when I felt the weight of my ‘impostor syndrome.’ Moose and Squirrel for life!

I would like to extend my heartfelt thanks to my advisor, Dr. Erik Melchiorre for his guidance. I literally would not have been able to be involved in this amazing project without you. Thank you, thank you, thank you for everything.

I also want to thank my committee members Dr. W. Britt Leatham, Dr. Codi Lazar, and Dr. Joan Fryxell for their support throughout my Undergraduate and Graduate careers at CSUSB.

This project would not have been possible without the work done by Bob Evans. I will forever be grateful for the opportunity to work with him on this project.

I would like to give a special thanks to Dwight Manleyfor letting me study this amazing historical treasure. This experience will be one that I cherish for the rest of my life.

I would also like to give a special thanks to Kenneth Domanik at the Lunar and Planetary Laboratory at University of Arizona in Tucson, AZ for assisting me in analyzing my samples, as well as the National Petrographic Service for assisting me in prepping my samples for analysis.

Lastly, I will never be able to express how thankful I am to all of my teachers throughout my academic career for sharing their knowledge and passion for geology with me. I would like to especially thank Professor Richard Hughes, III at Crafton Hills College for inspiring me to become a geologist.

DEDICATION

This work is dedicated to the love of my life, Justin Bowker. You inspire me every day to work hard. I am so honored to be by your side, and I am so excited for what the future will bring. I love you with all of my heart.

TABLE OF CONTENTS

LIST OF TABLES

LIST OF FIGURES

CHAPTER ONE

SS CENTRAL AMERICA - THE SHIP OF GOLD

Brief History

The keel of the SS George Law (later renamed the SS Central America) was laid in October of 1852 at Morgan Iron Works under the supervision of William H. Webb (Herdendorf, 1995). Webb's design called for two 85 m length inclined oscillating cylinder steam engines (a.k.a. wobblers), and a total of three decks to accommodate passengers and cargo (Herdendorf, 1995). Although it is often portrayed in illustrations as having two smokestacks, the steamer was only constructed with one (Herdendorf, 1995). The SS George Law entered service on October 20th, 1853 (Herdendorf, 1995).

The ship was originally named the SS George Law for the American financier who, along with Marshall O. Roberts and Bowes R. McIlvaine, established the US Mail Steamship Company (Herdendorf, 1995). The company formed in 1848 when awarded a contract from the United States government to carry US mails from New York City to Panama along its delivery route bound for California (Thompson, 1998).

The typical round-trip journey for the SS George Law began in the Port of New York. It ended in Aspinwall (Colón, Panama today), where passengers and freight bound for California would depart and board the Panama Railroad. In contrast, those on the return trip bound for New York were loaded onto the ship (Herdendorf, 1995). After a short layover in Havana for fuel resupply, the SS

George Law would return to New York to deliver passengers and goods (Herdendorf, 1995). The trip took roughly 20 days and consumed ~1200 tons of coal (Herdendorf, 1995).

Renaming to SS Central America

According to a Department of the Navy report, damage to the hulls of wooden ships from wood-boring bivalves (aka shipworms) native to Caribbean waters were commonplace (as reported in Herdendorf, 1995), and hulls were typically sheathed in thin copper plates to repel these animals. Throughout five years (1853-1857), the SS George Law underwent four “routine ship repairs,” which included repairs to the hull (Herdendorf, 1995). Repairs done June/July of 1857 included a re-coppering of the hull and an overhaul of the engines and boilers (Herdendorf, 1995). It was also at this time that the ship was renamed the SS Central America (Herdendorf, 1995).

Commander Herndon, USN

During its five years in service, the SS Central America completed 43 successful trips, carried over 13,000 passengers, and transported over $54 million worth of gold (based upon the 1857 price of $20.67 per troy ounce; 2.6 million ounces, or 81,250 kg) from California (Herdendorf, 1995). The ship had seven different commanding officers with Commander William Lewis Herndon, USN, a decorated Naval Officer, leading nineteen total voyages.

Commander Herndon was the final commanding officer of the SS Central America. The 43-year-old Virginia native had led an illustrious career in the

United States Navy (Herdendorf, 1995). In 1851, Commander Herndon led an expedition along the Amazon River (Herdendorf, 1995). Two years later, he filed his 414-page illustrated report to the Navy (Herndon and Gibbon, 1854) which was published the following year under the title “Exploration of the Valley of the Amazon” and became very popular with the public. Commander Herndon was also assisting his brother-in-law, Lieutenant Matthew Fontaine Maury (a.k.a. the Father of Modern Oceanography), in creating oceanic wind and current charts (Maury, 1855). Unfortunately, Commander Herndon opted to remain with the sinking SS Central America and oversee the evacuation of passengers; his heroic death deeply moved the country (Conrad, 1988). Commander Herndon’s legacy lives on today, and his memory is preserved by a statue, the Herndon Monument, built at the US Naval Academy (USNA, 2020).

Final Voyage of the SS Central America

Figure 1. Showing the route of the shipment of gold lost aboard the SS Central America. (Seymour, 2018)

The final voyage of the SS Central America (Figure 1) has been well documented both academically and among treasure seekers (Klare, 1992; Herdendorf, 1995; Kinder, 1998😉. The ship left port in Aspinwall, Panama, on September 3, 1857, with 476 passengers and an official shipment of gold valued over $1.2 million in dollars of the day (Herdendorf, 1995). For reference, gold was valued at $20.67 per ounce in 1857, which would translate to about 58,000 troy ounces. An unknown yet substantial quantity of gold was also brought in the baggage and on the person of returning 49ers. After staying a night in Havana for

refueling and supplying, the ship departed at 9:30 a.m. on September 8, 1857 (Herdendorf, 1995). The following day, a tropical storm began to develop over the Atlantic Ocean, which eventually turned into a Category 2 hurricane (Figure 2; Landsea and Franklin, 2013).

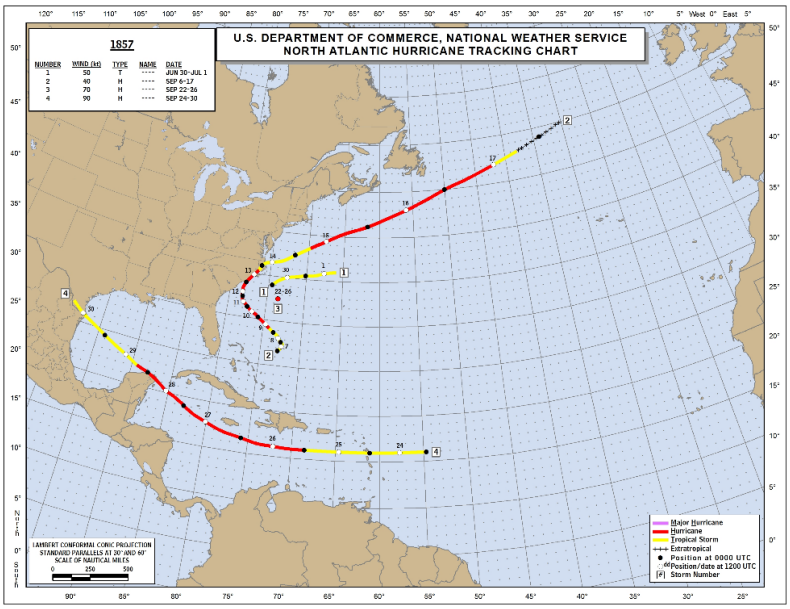

Figure 2. Showing the traces of hurricanes recorded in the Northern Atlantic in 1857 by the HURDAT2 program. Track 2 shows the hurricane responsible for the sinking of the SS Central America. (Landsea and Franklin, 2013)

The SS Central America floundered in hurricane conditions for two days, causing multiple leaks in the twisted hull (Herdendorf, 1995). For over 30 hours, the crew and passengers bailed the rising water that threatened to extinguish the boilers (Herdendorf, 1995). By the third day, the boiler room flooded and

extinguished the steam boiler fires. With coal wetted by seawater, there was no way to restart the boilers, eliminating power and the ability to control the ship in the storm (Herdendorf, 1995). Evacuation of the women and children began immediately, and by the night of September 12th, 1857, the SS Central America sat at the bottom of the Atlantic Ocean (Herdendorf, 1995). The sinking resulted in the loss of over 400 lives and the 15-ton shipment of gold in its cargo hold (Conrad, 1988; Klare, 1992; Herdendorf, 1995; Kinder, 1998). The loss of the gold shipment was a major blow to the United States economy and contributed significantly to the Financial Panic of 1857 (Klare, 1992; Herdendorf, 1995; Kinder 1998).

Rediscovering the SS Central America

The shipwreck site was finally discovered in 1986 by the Columbus American Discovery Group. With a team of salvage experts and scientists, the Columbus Group recovered materials from the wreck during a series of expeditions from 1986 – 1991. The shipwreck was discovered using historical data (i.e., reported coordinates from nearby vessels and wind and tide charts) combined with Search Theory and Composite Probability Maps to identify anomalies along the seafloor (Evans, 2018). Sonar was used to flag these anomalies, and the team selected Blake-Bahama Outer Ridge, a site 2200-m (1.37-mi) below the ocean's surface, to begin their investigation (Evans, 2018).

Blake Ridge

Blake Ridge is a 500-km long, 8.5-km thick sediment dune that slopes gently for about 300-miles and is “gently flushed” by the Deep Western Boundary Current (Evans, 2018; Herdendorf, 1995). The environment is described as calm, with abundant plant debris and undisturbed animal tracks (Herdendorf, 1995). When researchers first examined the site, they discovered the remains of a paddlewheel; a week later, they stumbled upon the famed Garden of Gold (Figures 3A,B) (Evans, 2018).

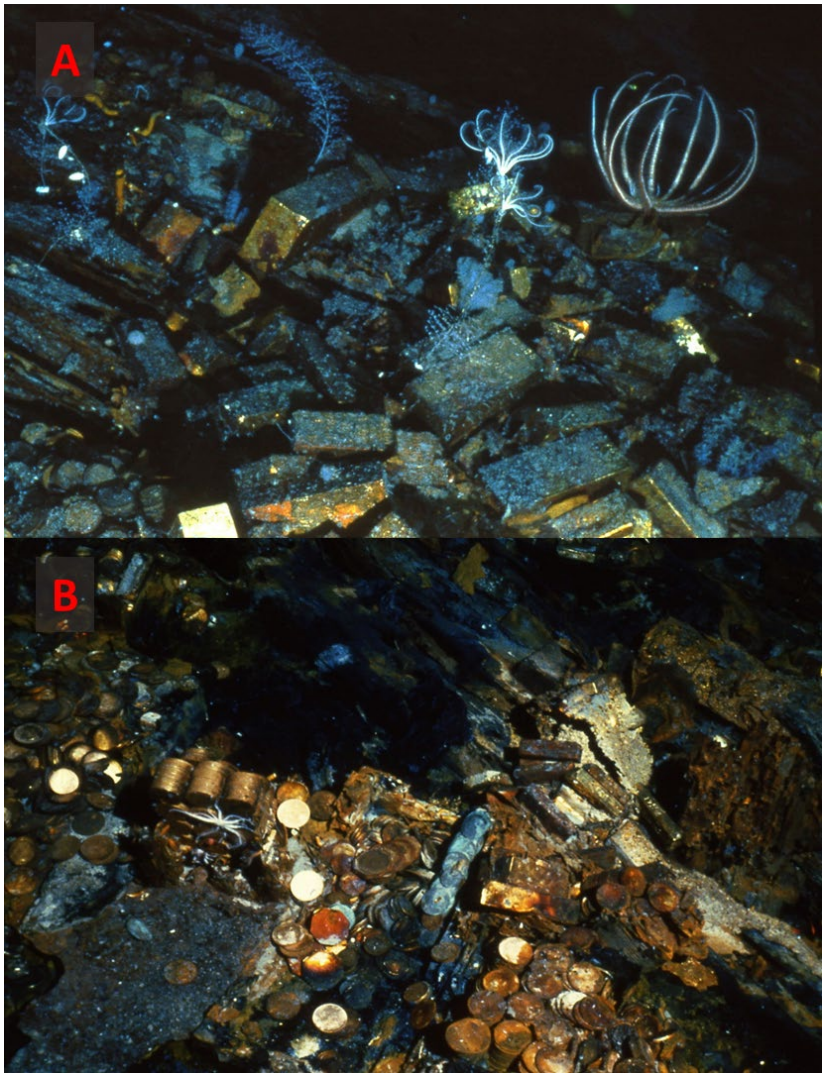

Figure 3. [A] Showing stacks of ingots along the sea floor surrounded by decaying ship timbers. [B] Coins were found in stacks, just as they had been placed in their wooden boxes when stored on the ship. (Evans, 2018)

2014 Expedition

In the 1990s, theDwight Manly purchased the Columbus American Discovery Group and its assets. In 2014, another expedition was sent to Blake Ridge to survey and excavate the 10-acre debris field surrounding the wreck

(Evans, 2018). The newer, updated technology allowed for the collection of more data in two weeks that the whole original excavation season (Evans, 2018).

While surveying the debris field, the team came upon the ship purser's safe (Evans, 2018). The ship's purser was an officer who acted as an accountant for the crew and was in charge of keeping the ship stocked with equipment and food, as well as keeping track of everyone's pay (USS Constitution Museum, 2011). After sitting on the ocean floor for over 150 years, the safe was still intact (Figure 4A; Evans, 2018). When the team attempted to move it, the door fell off, revealing a bag of silver dimes, a saddlebag, and a vest rolled in a bundle and wrapped in twine (Figure 4B; Evans, 2018). Later research showed that the vest was not on the ship's manifest (Evans, 2018). The fact that it was found in the ship's purser safe was even more puzzling.

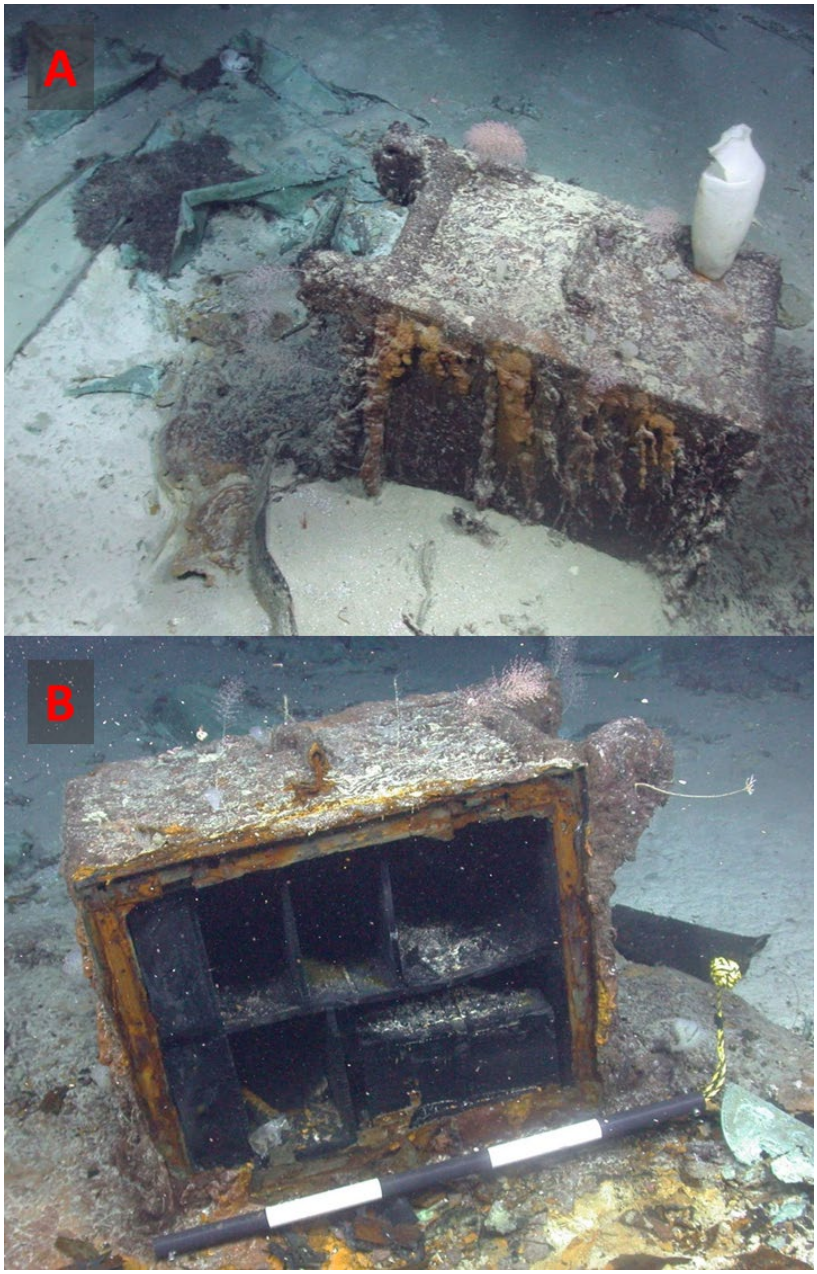

Figure 4. [A] Purser safe found in the debris field surrounding the shipwreck. [B] The safe's door broke off as scientists tried to examine the safe. (Evans 2018)

In the summer of 2018, I had the privilege of meeting Bob Evans at his laboratory to witness the opening of one of the pokes recovered during the 2014 expedition. To preserve the artifacts, they were kept in plastic containers filled with seawater (Evans, 2018). In total, four pokes were recovered from the vest (Evans, 2018). Pokes 1 – 3 were made of leather, while Poke 4 was made of canvas (Evans, 2018). Poke 2 has the name “L. Darcey” written along the side of it, while Poke 4 has illegible text written along its corner (Evans, 2018).

CHAPTER TWO:

CALIFORNIA'S GOLD RUSH - THE EARLY YEARS

"Gold Mine Found"

The history of California's gold rush began in January of 1848 when James Marshall discovered gold in the tailrace of the sawmill he was overseeing the construction of near Sutter's Fort (present-day Coloma) along the American River (Coloma, 2020; Encyclopedia Britannica, 2020). News of the discovery quickly spread when The Californian, a newspaper printed in Yerba Buena (present-day San Francisco, California), declared "Gold Mine Found" in an article published on March 25th, 1848 (Museum of the City of San Francisco, 2020). As more reports confirming the find surfaced, gold seekers literally dropped what they were doing and made for the hills to seek their fortunes (Coloma, 2020; Herdendorf, 1995; Museum of the City of San Francisco, 2020).

During the early years of the Gold Rush, gold-seekers worked along the banks of streams in placer deposits to extract the coarse gold, and, in some locations, the gold was picked up right off the ground. A placer deposit is unconsolidated to weakly consolidated sediments which contain economically minable concentrations of valuable dense minerals such as gold, which have been concentrated by the action of water or wind. Within a few years, techniques to extract the finer gold were quickly developed and implemented (Sierra College, 2009). As production from placer deposits along active waterways waned, prospectors turned their attention to the surrounding hillsides. Although

hydraulic mining equipment was first experimentally used in California in the early 1850s to wash whole hillsides of their gold-bearing gravels (Sierra College, 2009), these techniques were not “widely” used in the region until the 1860s with the rise of larger companies (Kelley, 1954). Hydraulic mining abruptly ended in 1884 when the Sawyer Decision led to the closing of many mines in the Sierra Nevada region (Kelley, 1959). Much has been written about this period of California history, and more details can be found in many places including Lindgren, 1911; Oakland Museum of California, 1998; Coloma, 2020; and Museum of the City of San Francisco, 2020.

Traditional Mining Techniques

Placer deposits are commonly mined along river valleys as these deposits can be easily found and exploited with minimal equipment (Silva, 1986). Before the development and widespread use of hydraulic mining (a.k.a. hydraulicking) in California, early miners used basic gravity separation techniques to extract placer gold from river deposits (Silva, 1986).

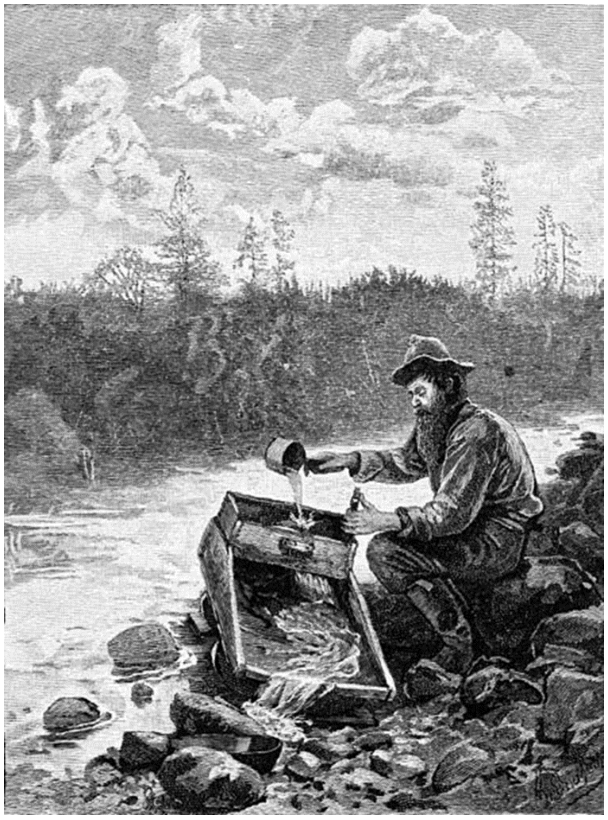

Figure 5. “The Cradle”, Showing a prospector working a placer deposit using a rocker sluice. This illustration was published in The Century illustrated monthly magazine in Jan 1883. (Sandham, 2016; public domain)

Individual prospectors would work high-grade areas or areas along the inside bends of rivers where gravity and water had naturally enriched the concentration of gold. They used a small sluice called a rocker or cradle (Figure 5) in which they separated the gold from river sediments. These sluices would be set in pre-dug groves in the ground in such a way as to allow running water to carry away the unwanted lighter material and leave behind the denser gold and black sands. The material caught in grooves along the bottom of the sluice was

transferred into a pan (Figure 6) where the gold was further separated from the black sands.

Figure 6. Showing a prospector separating gold from black sands using a gold pan. (Author's photo)

As more and more prospectors arrived and worked the land, most of the more easily accessible surface gold deposits were quickly exhausted (Hank, 1884). Prospectors now had to find economical ways of extracting the vast

amounts of fine-grained gold from river sediments. The increase in work needed to remove the gold led most prospectors to form small companies of 10 – 15 workers. With some pioneer ingenuity and elbow grease, the groups would completely dam up and divert rivers to allow easier access to deposits along the former river bottom. The increase in waste material caused prospectors to abandon their pans and rockers for larger equipment that could process more material, faster.

Figure 7. “The Sluice”, Illustration showing miners feeding material into a long tom sluice (uppermost worker with shovel) and removing larger rocks with a “sluice fork” (right-side worker). This illustration was published in The Century illustrated monthly magazine in Jan 1883 (Sandham, 2010; public domain).

As companies expanded, the available technology needed to adapt to accommodate the increase in material that needed to be processed. In response to the increase in production, long toms (Figure 7), or rockers that had been expanded to have up to 20-foot troughs (Sierra College, 2009), were developed. Long toms always needed to be supervised, as they require a constant supply of moving water to wash away the gangue material (Sierra College, 2009). Flumes were constructed and acted as artificial waterways to bring water to the areas where running water was not readily available (Baumgart, 2009).

Figure 8. Small beads of mercury (shown in the red box). Some of the free mercury left at the bottom of sluice would often be washed away. Today, mercury contamination can be found in most locations throughout the Sierra Nevada Mountains. (Author's photo)

Some more successful companies also began utilizing mercury (Hg) amalgamation (Figure 8). Mercury would be put in the riffles of sluices to absorb fine gold. In this process, the liquid metal mercury melts the fine-grained gold and forms a new liquid mercury-gold alloy (Hank, 1884). Experiments conducted by Hank (1884) showed that placer gold of California was commonly coated in sesquioxide of Fe. This “dirty” gold was seen to be “perfectly inert to the action of mercury” and would essentially “float on the surface” being easily detached during “placer washing” (Hank, 1884). However, clean gold would easily amalgamate with mercury (Hank, 1884). As the gold content of the mercury-gold alloy increased, it approached its room temperature freezing point and became stiff (Hank, 1884). This frozen amalgam would be collected and heated in a special type of still, called a retort. The heating drove off the mercury and collected it for reuse, leaving behind a spongy mass of gold.

By the 1860s, the costly nature of extracting the fine gold and gradual depletion of richer gold placers eventually caused a lot of small companies to sell, which allowed larger companies to purchase land surrounding their properties. Hydraulic mining and later dredge boats began exploiting the marginal but large volume placers in this period. It was in this same period that hard-rock mining of the quartz-gold deposits of the Mother Lode began in earnest.

Using the Right Equipment for the Job

Throughout the Gold Rush, prospectors practiced various techniques in order to recover the most amount of gold. Depending on the prospector's proximity to running water, they would employ wet and/or dry gravity concentration techniques.

Table 1. Showing the distribution of grain sizes recovered from specific Gravity Concentration techniques available during the California Gold Rush. (Modified from Mildren, 1980)

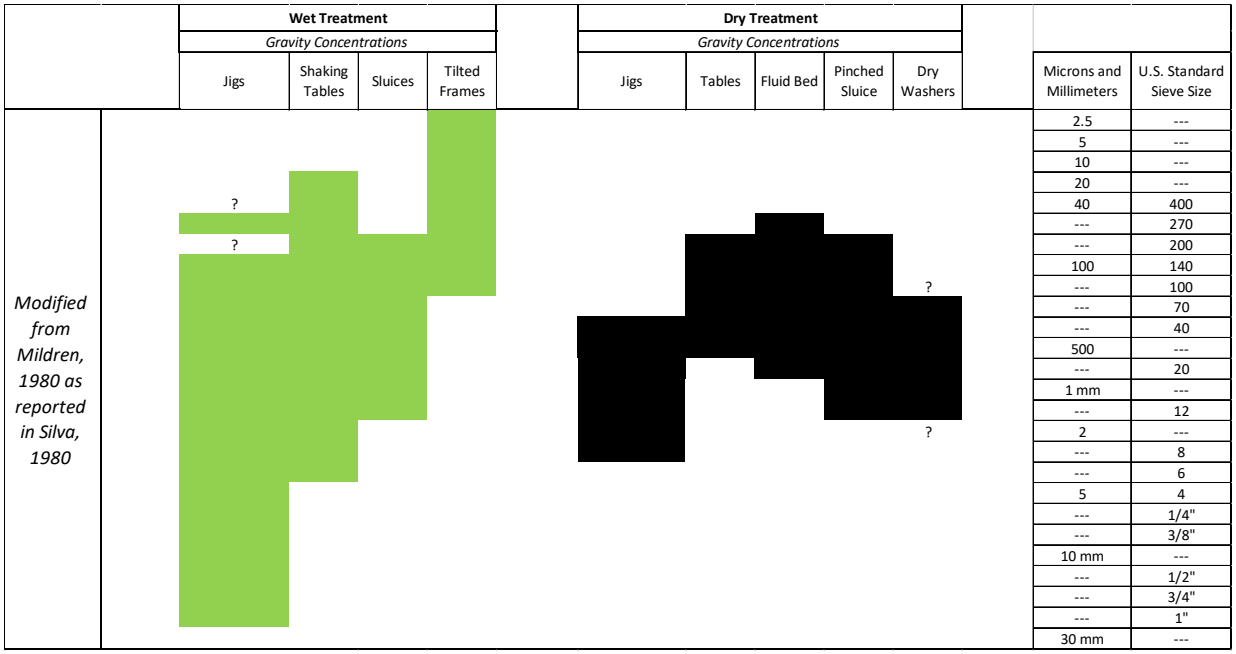

As can be seen in Table 1, different mining methods have different recovery rates and particle sizes. For example, dry washing methods do not

recover very fine-grained gold (i.e., ≤40 microns), and are only employed where water is unavailable in quantity. Conversely, modern tools such as vibrating jigs and spiral wheels can recover very fine-grained gold, but often miss larger oversize gold that is screened off. Of the techniques that would have been in common use during 1857 (sluices and rockers), a wide range of gold particle recovery was possible. With the addition of liquid mercury in the riffles of a large sluice complex, additional fine gold could be recovered. However, only large companies could afford the high cost of importing mercury during the early years of the gold rush.

California gold production of the period 1856-1857 was dominated by placer mining by small companies and saw the waning days of the solitary prospector. Production was chiefly made using the long tom sluice operated by small groups of 5 to 15 miners. Expensive mercury was used when local conditions (i.e., proportion of fine gold in the deposit and mineral coatings on the gold) were favorable and the group could afford the expense. These types of operations would recover a wide range of gold particles sizes. The presence of fine gold (<1mm) indicated operations that did not directly employ mercury or restricted its use for economic reasons to the lower-most sluice riffles.

While the Mother Lode bedrock source of the placer gold was known by this time period, there was little lode gold mining. Hard rock mining is much more expensive and dangerous than placer mining, and typically requires a large company that can construct the infrastructure to mine and extract the gold from

bedrock. The minor lode gold production of this period was mostly limited to shallow prospect pits along heavily weathered and oxidized surface ore.

CHAPTER THREE:

GEOLOGIC SETTING - WESTERN SIERRA NEVADA FOOTHILLS

Overview

The entire western margin of the North American Plate, notably California, was formed as the result of a subduction zone that sat offshore for 10s of millions of years during the Mesozoic Era (Harden, 2004). The Farallon Plate, composed of oceanic crust, was thrust underneath the North American Plate, which is composed of continental crust (Harden, 2004). As island arcs (or chains of islands) on the Farallon Plate met with the North American plate, they were accreted onto the side of the continent, adding more real estate to the landmass (Harden, 2004).

It was after one of these major accretion events (late-Jurassic, about 155 ± 3 Ma) that the Nevadan compressional event occurred which created the widespread fault displacement found throughout the western Sierra Foothills (Lindgren, 1895; Schweickert et al., 1984; Böhlke, 1999). These major fracture zones, dubbed the foothills fault system (Böhlke, 1999), provided the pathways for a massive complex of quartz+gold+base metal sulfide veins (now called the “Mother Lode”) to be injected along fractures in the granitic and metamorphic bedrock of the western Sierra Nevada Mountains.

Lindgren (1895) and others have argued that the quartz-gold veins, themselves, are the results of the interaction between the large, Mesozoic-aged

magma body (and its associated mineral-rich fluids) along the western coast of North America and the metamorphic country rock of the Sierras. At a subduction zone, a significant amount of seawater enters the subduction zone and lowers the melting point of local rocks, creating large bodies of magma. The hotter magma can melt more of the surrounding country rock and incorporate it into its magma body; this includes deposits that the magma may not have been able to melt at its original temperature and water content. The hot, mineral-rich water (called hydrothermal fluid) associated with the magma body works its way up to the surface through any weakness it can find; in the case of California, the contact zones between accreted terranes were ideal. Along its pathway, the hot waters can dissolve silica, gold, and other minerals. As the hydrothermal fluids rise and cool, they precipitate their dissolved load within the fracture pathway, creating the veins of quartz+gold+base metal sulfides.

Not all scientists agree with Lindgren's (1985) hypotheses about the origins of the quartz-gold veins of the California Mother Lode. Sibson et al. (1988) argued that the veins may represent sporadic routes of escape for hydrothermal fluids trapped near the brittle-ductile transition zone (as reported in Böhlke, 1999). Cloos (1935) suggested the fracture zone is the result of the thrust faulting along the margins of magmatic intrusions (as reported in Böhlke, 1999). Landefeld (1988) argues that the influence of local magmatic activity is minimal and that the fracture zones were the result of regional lateral movement occurring at the same time as mineralization (as reported in Böhlke, 1999).

Although the exact mechanisms are still debated among scientist, all generally agree that the quartz-gold veins were deposited by a carbonaceous hydrothermal fluid that worked its way through fractured zones, geochemically altering the rock as it moved. The elevated flux of heat through the local bedrock created massive hydrothermal circulation cells, which dissolved quartz and traces of gold. In their upward path along fractures, these hot waters cooled and as they lost their ability to contain dissolved solids, formed a network of large gold-quartz veins that as a group are called the “Mother Lode” (Lindgren, 1895).

Quartz-Gold Veins of the Mother Lode

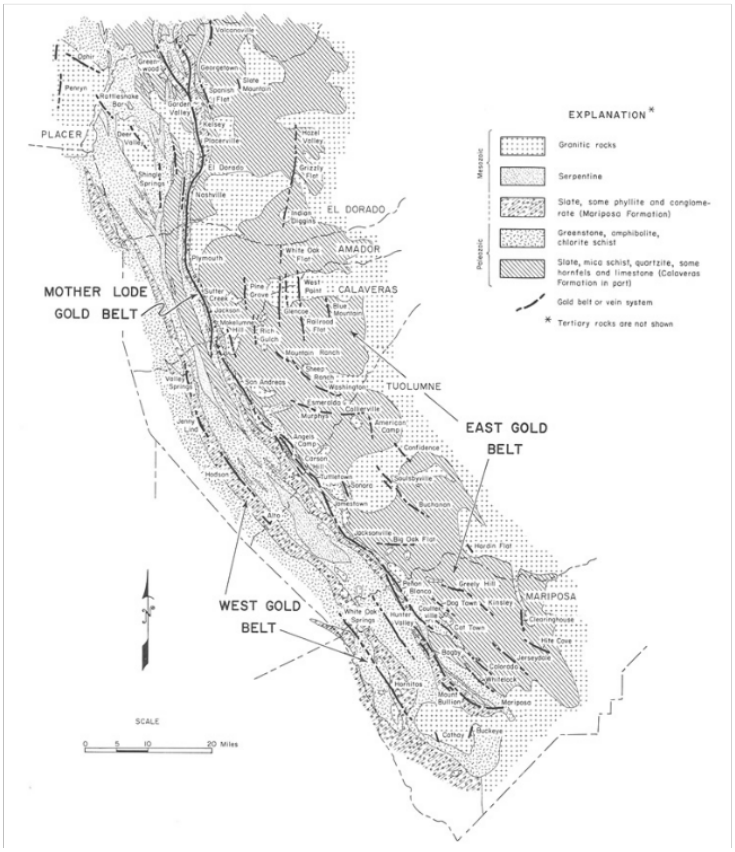

Figure 9. Map showing the location of the Mother Lode belt in the western Sierra Nevada foothills (Source: Harper, 2012; public domain).

The quartz, auriferous-bearing veins of California's Mother Lode Country are located on the western side of the Sierra Nevada mountain range (Figure 9) in predominantly metamorphic rocks (Lindgren, 1895; Turner, 1894). The quartz-gold veins of this area are characterized as "fissure" veins (Lindgren, 1895). As the country rock was experiencing an immense amount of compressive stress from plate tectonics, fissures began to develop throughout its structure (Lindgren, 1895). These included a single, large fracture or a grouping of several fractures,

all of which may extend for only a few miles (Lindgren, 1895). Although the fissures tend to follow the foliation planes of the rock's they crosscut, the influence of the country-rock on the vein's characteristics is minimal (Lindgren, 1895). A generalized description of the veins' attitudes is beyond the scope of this study as they vary from mining district to mining district. The largest concentrations of gold are found where multiple veins intersect; these are known as pocket veins (Lindgren, 1895).

In a presentation before the Geological Society of America (GSA), Lindgren (1895) described the generalized 3-step process of the deposition of the quartz-gold veins in the Mother Lode as follows:

1) The carbonated, hydrothermal fluids altered the soluble minerals in the country-rock.
2) As the process finishes, the "walls" are coated with carbonate crystals.
3) The free silica, along with the native gold and metal sulfides, begins to deposit in the area surrounding the carbonates.

Later studies showed a "clear spatial association between gold-quartz veins and some major NW-SE trending fault zones in metamorphic belt… [including] significant regional association of gold-quartz veins with serpentine" (Böhlke, 1999). A study by Seward (1991) supported "gold transportation by aqueous sulfide complexes… [and] precipitation from solution from a combination of cooling, mixing, degassing, sulfide precipitation, and increasing or

decreasing fluid pH or oxidation state" (as reported in Böhlke, 1999). However, a study by Böhlke and Kistler (1986) using hydrogen isotope data "indicated serpentization and carbonate metasomatism were accomplished independently by fluids from different source." Böhlke (1999) also indicated that "some Sierran gold vein systems are disseminated deposits associated with pyrite formed in the wall rocks by metasomatism by the same types of fluids that formed the veins." Böhlke (1999) further suggests that "associations of disseminated gold with pyrite indicate that rock sulfidization and consequent fluid desulfidization may have caused gold to precipitate locally from saturated solutions containing gold-bisulfate complexes."

Minerals Associated with the Veins. Other minerals found in the gold-quartz veins include calcite, magnesite (rare), dolomite, muscovite, roscoelite (rare), rhodonite, albite (rare), titanite, ilmenite, and anatase (Lindgren, 1895). The most common mineral group associated with these veins are the sulfides: Fe-pyrite (very common), Cu-pyrites (common), and pyrrhotite (rare). (Lindgren, 1895). Also, compounds of arsenic, antimony, and tellurium occur in some places (Lindgren, 1895). There have been cases of mariposite and platinum-group minerals being associated with placer Au deposits. However, they are not associated with the quartz-gold veins; they are simply found in abundance in surrounding deposits and end up together in the placer sediments (Lindgren, 1895).

Rock Types

The bedrock types that host the quartz-gold veins include granite, diorite, granodiorite, gabbro, serpentine, quartz-porphyrite, augite- or hornblende-porphyrite, diabase, amphibolite and other metamorphic rocks, as well as altered slates, sandstones, and limestone (Lindgren, 1895). Occasionally, near rich ore shoots, native gold deposits occur in the country-rock (Lindgren, 1895). The ore shoots were found “preferentially in areas of intense and late fracturing, near vein intersections, and along certain types of lithologic boundaries” (Böhlke, 1999). Later petrographic studies “indicate that gold and most closely associated sulfides… were deposited relatively late in the sequence of vein filling phases” (Böhlke, 1999).

Alteration

Early studies of the alteration zones of country rock, or the zones on either side of the quartz veins, revealed that the primary type of alteration was "carbonatization… [or] the conversion of the country-rock to carbonates" (Lindgren, 1895). The auriferous-bearing hydrothermal fluid altered the rocks with different intensities depending on the host rock's chemistry (Lindgren, 1895). For example, nearly all igneous rocks, basic and acidic, were found to have undergone significant alteration, particularly to produce minerals of the serpentine group (Lindgren, 1895). On the other end, rocks with a high silica content, particularly carbonaceous slates, were found to have the least amount of alteration (Lindgren, 1895). The alteration zones often contain carbonates, sericite, some chloritic minerals, residuary quartz (including ones that are partly chalcedonic), lots of Fe-pyrites, and some As-pyrites (Lindgren, 1895).

Later studies, using electron microprobe analyses and x-ray diffraction confirmed the presence of products of carbonate metasomatism associated with the gold-quartz veins (Böhlke, 1988, 1989, 1999). The carbonate metasomatism evidence was most abundant in mafic and ultramafic rock (Böhlke, 1988, 1989, 1999). Böhlke (1988) also suggested that "gold could be released by reaction of Mother Lode-type CO_2-rich fluids with gold-bearing sulfide minerals in rocks with less than average Fe/Mg ratios."

Hydrothermal Fluids

Early on, Lindgren (1895) hypothesized that the hydrothermal fluids responsible for the deposition of gold in the western Sierra Nevada foothills are thought to have a basic chemistry of “water with free silica, carbon dioxide, dissolved Ca-carbonate, dissolved Na-carbonate, silicate, chloride, and sulfur… [including] sulphuretted hydrogen or as sulpho-salts.” Hydrothermal fluids of this chemistry are “known in nature as ascending, usually hot springs” (Lindgren, 1895).

Today, the origin of the hydrothermal fluids responsible for the deposition of the quartz-gold veins is hotly debated; however, most scientists agree that the major ingredient was carbonic acid (Böhlke, 1988, 1989, 1999). In support of Lindgren’s hypotheses, Böhlke (1988) argued that “on the basis of thermodynamic evidence… carbonatization reactions involving dolomite-ankerite and magnesite-siderite solid solutions in a variety of wall rocks precluded a local source of fluid CO_2.” Based on hydrothermal experiments, thermodynamic analyses, and fluid inclusion studies, Böhlke (1999) suggests that this indicated that “aqueous sulfide species may have been largely responsible for the solubility of the gold… [the] low chlorinity and low acidity of the fluids may have precluded transport of much larger quantities of base metals.”

Placer Gold Deposits

The lode deposits of the Mother Lode were still deep underground when the Farallon Plate was completely subducted (Harden, 2004). It was at this time

(~30 Ma) that the Pacific Plate came into contact with the North American plate, and the San Andreas Fault was formed (Harden, 2004). The series of global cooling events (a.k.a. Ice Ages) during the Cenozoic brought continental glaciers that dramatically altered the landscape of Mesozoic and early Cenozoic eras (Harden, 2004; Lindgren, 1911). The giant fluvial systems associated with the melting of these glaciers connected water bodies from the Mojave Desert to the Pacific Ocean (Harden, 2004). The combination of steep terrain, glacial activity, and increased runoff deeply eroded the Sierra Nevada Mountains, exposing the quartz-gold veins and shedding gold into the sediments on slopes and in rivers (Harden, 2004). These fluvial deposits of California related to the last Ice Age are referred to as Tertiary Gravels and are some of the most famous auriferous-bearing gravels in the world (Lindgren, 1911). The later erosion of these Tertiary Gravels formed very rich secondary placers in modern stream channels (Lindgren, 1911).

These Tertiary gravels represent material deposited during multiple transgression/regression cycles from the late-Cretaceous (Pre-Chico) to the early-Quaternary (Sierran period) (Lindgren, 1911). In his landmark paper, Lindgren (1911) classified the Tertiary gravels of the western Sierras into six groups.

- Deep gravels (Eocene): “depth of 50 to 200 feet by coarse gravels which ordinarily have been cemented… large and well rounded… range in size up to cobble-stones and even bowlders [sic] several feet

in diameter… unless subsequently decomposed, [all] have a smooth or polished surface… there is no clay and the cementing material between the pebbles consists of coarse sand”

- Bench gravels (Miocene): “covering the deep gravels… pebbles are smaller and… well rounded and polished… a maximum thickness of 300 feet… in places… a width of 1 or 2 miles”
- Rhyolitic tuffs: “flows of white rhyolite, accompanied by large masses of rhyolitic tuff, of clayey and sandy character, covered the bench gravels… much of this tuff is in the mining region designated as pipe clay or chalk… flows attain on the idle slopes a maximum depth of about 200 feet; higher up they are much heavier”
- Gravels of the rhyolitic epoch: “the rhyolitic flows had the effect of damming many lateral streams, thus causing immediately accumulations of gravels, clay, and sands… detrital masses of gravel, sand, and clay, generally of a finer character than the bench gravels… [can] attain a thickness of several hundred feet”
- Andesitic tuffs and tuffaceous breccias: “only near the summits… are massive flows and breccias found… over the greater part of the slope the eruptions assumed the form of mud flows, at first as sandy and clayey masses but later mixed with a great quantity of larger angular or subangular fragments… thickness… usually less than 200 feet along the valley border… middle slopes the average thickness is about 500

feet… high on the range… a thickness of 1000 to 1500 feet was attained”

- Gravels of the andesitic epoch: “between the various flows the rivers continued their work and deposited gravels… sharp V-shaped canyons were cut through the older beds and in some places even down into the solid bedrock to a depth of about 100 feet”

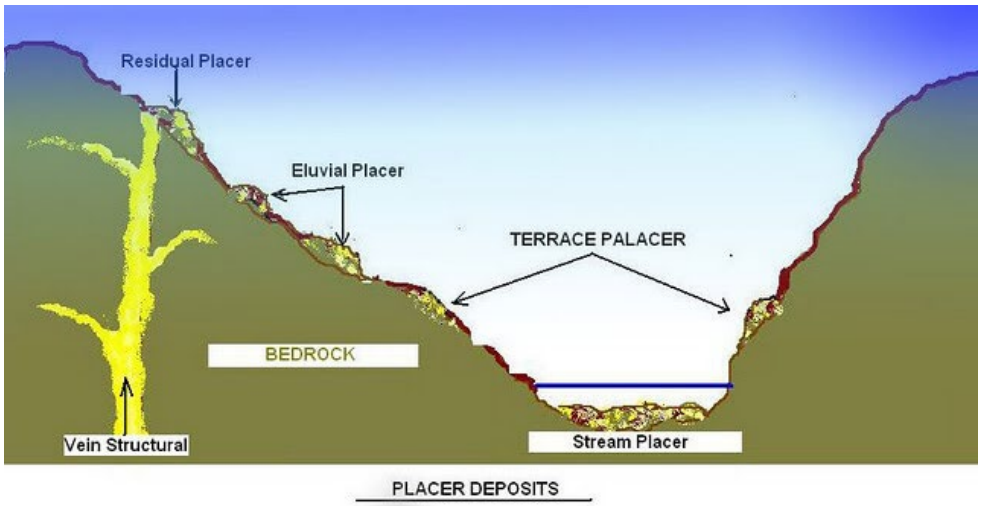

Figure 10. Diagram showing the locations of placer deposits (911 Metallurgist, 2016; public domain).

The modern gravels of the active drainage network of the Sierras have remobilized material from the Tertiary Gravels and re-concentrated their gold through the action of water. This produced exceptionally rich unconsolidated gold

bearing gravel deposits at bends in rivers, point bars, natural bedrock riffles, and waterfall potholes (Figure 10).

The modern placer deposits of California contain pockets of dense minerals, including gold. Locally, the suite of dense minerals (black sands) associated with the gold can vary and be indicative of a specific locality. For example, native platinum-group metal grains are found in placers of the Yuba River (Sjoberg and Gomes, 1981) . Other minerals, such as magnetite, are ubiquitous in all placers.

It was these modern alluvial deposits that were first mined in the California Gold Rush. Anyone with a modest appreciation of how water moves sediment and traps dense minerals with gravity could predict likely spots for gold accumulation. Once a rich deposit was discovered, their unconsolidated nature makes them easy to mine and process with simple hand tools. It was this type of deposit and style of mining that dominated the first decade of gold mining in California. As the decade wore on, the richer deposits became harder to find and miners banded together to pool their labor to economically exploit lower and lower grade gravels. It was in these waning days of the early gold rush that the placer gold from the SS Central America was mined.

The discovery of the gold-bearing Tertiary Gravels breathed new life into the gold rush in the early 1860s. Capitol-intensive infrastructure such as dams, extensive water flumes, and water cannons were funded by larger companies to

extract gold from the Tertiary Gravels through economy of scale. Significant amounts of gold were won by these methods, but only after 1860.

CHAPTER FOUR:

PREVIOUS WORK

Motivating Question

The primary motivating question behind my research is, who owned this vest? Was it an individual prospector that had gotten lucky and was on his way home? Was it a gold buyer that was taking samples back to their main office?

To answer this question, I needed to start with where this gold was collected. What we do know is that at this point in history, the mining towns of California's Mother Lode were the only gold producing districts of significance in this part of the country (Clark, 1970; Hanks, 1884; Lindgren, 1911). Also, all the passengers aboard the SS Central America were from California (Evans, 2018; Thompson, 1998). These two factors narrowed my study area to the western Sierra foothills of California.

This research aims to determine the geochemical and morphological make-up of the gold from these pokes and compare these findings to known mining locations from 1857 in California. Using X-Ray Fluorescence (XRF) analysis, scanning electron microscope (SEM) imaging, and Energy Dispersive Spectral analysis (EDS), I measured the shape and purity of the recovered placer gold. I also determined the composition of any inclusions and accessory minerals that may be present.

Previous Work

A study conducted by Herdendorf (1995) is the major scientific work undertaken on the SS Central America shipwreck. This 200+ page special volume comprises research from multiple disciplines, including marine biology, oceanography, and material science. The only other previous scientific study focused specifically on the mineral crusts and nano-particulate gold found growing on portions of the SS Central America gold cargo (Melchiorre et al., 2019). However, no scientific studies have been done specifically on the placer gold recovered from the SS Central America.

However, significant work has been done to evaluate the use of morphological and geochemical fingerprinting to determine the provenance of placer gold from many different locations around the world (e.g., Canada, Knight et al., 1999; New Zealand, Craw et al., 1999; Arizona, Melchiorre et al., 2017).

CHAPTER FIVE:

METHODOLOGY

Gold Purity

Non-destructive elemental abundance tests can be made on placer gold using X-ray fluorescence (XRF). The advantage is that this method does not destroy or alter the original sample, but it is limited to measuring the chemistry of the gold to only a few 10s of microns deep into the sample. Thus, to measure gold purity more accurately, the samples needed to be deeply polished, to expose the core of the gold grain. This permits detailed examination of chemical zonation and identification of mineral inclusions within the gold grain but destroys about half of the sample. My samples were sent to National Petrographic, a company that specialized in prepping samples for these types of laboratory tests.

The only way to measure the true purity of the gold is to measure the composition of its core. Like most things, gold exposed on the earth's surface undergoes various weathering processes. These processes slowly breakdown the gold, removing more soluble "impurities" such as silver and copper first. As a result, a simple analysis of the surface of deeply weathered gold would reveal a higher purity than the original gold; this is because the differential chemical weathering produces a gold enrichment at the outer surface. This phenomenon is well documented and called depletion gilding (Melchiorre et al., 2017). The core of the gold, which represents the original lode deposit chemistry of the gold, is generally less pure than its weathered rims. No natural gold is 100% pure gold; it

will always have some percentage of Ag and/or Cu in its alloy (and possibly some other accessory elements).

Gold samples showing concentrations of accessory minerals in their rim but not in their cores suggests that they were secondary deposits acquired by the hammering of these minerals into the soft gold during violent fluvial transport.

Gold purity was calculated using the following formula:

$$[(\%Au)/(\%Au+\%Ag+\%Cu)] \times 100 \quad \text{[Equation 1]}.$$

Gold Districts of California

The gold districts used in this study were defined using the same methodology as Hanks (1884). The data set also includes data from Clark (1970) and Lindgren (1911). See Appendix A for a full breakdown of the gold purities reported from each district. The following is a brief overview of the gold districts included in the Mother Lode region of California, as well as the average purity of gold found in each district (Hanks, 1884):

- Amador County: 90.5%
- Butte County: 90.9%
- Calaveras County: 89.1%
- El Dorado County: 88.0%
- Nevada County: 88.1%
- Placer County: 89.3%

- Plumas County: 89.8%
- Sierra County: 89.4%
- Tuolumne County: 88.2%
- Yuba County: 93.3%

Modern Comparative Data

Due to restrictions in place from the COVID-19 pandemic, I was unable to collect samples of modern gold from the above localities directly in the field. In lieu of collecting samples, my advisor purchased gold samples collected from the Yuba and Feathers rivers from Natural Gold Trader, LLC (Figures 11a and 11b, Table 2). Their analyses were performed by Dr. Erik Melchiorre. A full breakdown of the geochemical analysis of the gold can be found in Appendix B.

Figure 11a. Yuba River gold.

Figure 11b. Feather River gold.

Table 2. Gold purity of samples collected from Yuba and Feather rivers.

River/Sample #	%Au	%Ag	%Cu	Au Purity
Yuba1	91.468	0.083	0.048	99.86%
Yuba2	80.071	0.244	0.087	99.59%
Yuba3	73.851	0.158	0.072	99.69%
Feather1	59.178	3.692	0.022	94.09%
Feather2	71.390	3.538	0.015	95.26%
Feather3	64.374	4.680	0.027	93.19%

Major and Minor Element Chemistry

XRF was used to non-destructively analyze larger placer gold samples. These samples were analyzed for major and minor element chemistry using a NITON XRF GOLD+ instrument operating in the Cu/Zn Mining Mode, with a dwell time of 240 seconds. A full description of this methodology is provided in Melchiorre et al. (2017).

Smaller placer gold samples were mounted on double-sided carbon tape on an aluminum post mount for Scanning Electron Microscope/Energy Dispersive Spectral (SEM/EDS) analysis. Samples were arranged on their flattest side to expose the maximum surface area and photographed under a binocular microscope or SEM as dictated by particle size. A Phenom XL SEM was used to capture Secondary Electron (SE) and Backscatter Electron (BSE) images using an acceleration voltage of 2 kV or 15 kV, respectively.

The Phenom XL SEM was also used for EDS measurements of major and minor element abundances, using standard off-peak interference and matrix corrections (Armstrong, 1988; Donovan et al., 1993), and calibrations using registered standards provided by the manufacturer. The error associated with the in-situ trace element EDS analyses is less than ±2%.

Following analyses of grain surfaces, some samples were embedded in epoxy and polished to expose the interior of the gold grains. Additional SEM/EDS work was done as above, to examine any internal variation in gold alloy chemistry and inclusion types. Detailed microprobe work was done on these

samples in the Lunar and Planetary Laboratory at University of Arizona in Tucson, AZ using a Cameca SX 100 Electron Probe Microanalyzer.

Inclusions

Inclusions are minerals that occur within the structure of the placer gold. The inclusions found in the core of the gold grains are typically interpreted as having formed with the gold in the lode source. Inclusions found only in the outer surface of the gold are typically interpreted as having accumulated during sediment transport. Analysis of these gives us insight into the conditions of the hydrothermal fluid the gold formed from and the path of the gold during transport. Some inclusion minerals are ubiquitous and can be found almost anywhere on earth, while others are limited to specific locations.

Accessory Minerals

Accessory Minerals, commonly called “black sand,” represent the other minerals that are a part of the fluvial system the gold was collected from. Even for a seasoned prospector, it is inevitable that you will end up with some traces of black sand with your gold. These are often other “dense” minerals that get trapped in the same gold recovery process. Some black sand minerals such as magnetite are widespread and can be found in almost every waterway in the western Sierras, while others are rare minerals limited to specific locations. The degree of wear and rounding of magnetite crystal octahedron is often used as an informal gauge of transport distance.

Morphology

The morphology of the gold can help determine where in a fluvial system the gold was collected from. Native gold is very soft and, therefore, malleable. It has a hardness of 2.5 on the Mohs hardness scale; this is the same hardness as our fingernails. As the process of saltation moves the gold down a river channel, the gold's shape is altered. Gold has a very high density (19.32 g/cm^3). If a fluvial system has enough energy even to pick up a gold nugget, then it is going to have a hard landing at the end of its jump—each impact "dents" the gold, altering its original shape. Rounded, more flat gold represents gold that has traveled along a fluvial system for a significant distance. In contrast, more angular, crystalline gold nuggets represent gold that was collected closer to its source.

The morphology and geochemistry of individual placer gold grains were imaged and measured using methods described in Shuster et al. (2015). Measurement of placer gold dimensions was performed with a microscope sample grid or SEM scale. The longest axis was measured as "length," the longest axis perpendicular to this was measured as the "width," and the short axis perpendicular to the previous two was measured as "thickness." These dimensions are expressed as width/length versus thickness/width ratios using the methods outlined by Zingg (1935) and Blott and Pye (2008) to understand their possible transport history and provide a morphological fingerprint. These dimensions were also used to calculate the flatness index (FI) of the grains to

determine the distance they were collected from their source rock using the method outlined in Cailleux and Tricart (1959) and Hérail et. al. (1990).

Zingg Diagram

A Zingg diagram is used “to plot ratios of breadth to length… and thickness to breadth” (Blott and Pye, 2008). These ratios, expressed as S/I and I/L are plotted on a bivariate diagram and are expressed as four different classes that translate to “flat, spherical, flat and columnar, and columnar” (Blott and Pye, 2008).

Elongation, Flatness, and Particle Form Diagrams

The diagrams outlined in Blott and Pye (2008) are modified versions of the Zingg diagram to show a more detailed version of the morphology of particles. Blott and Pye (2008) argue that “particle form can be described simply in terms of deviation from equancy in just two respects, elongation and flatness (i.e., by the I/L ratio and by the S/I ratio, respectively).”

For the Elongation diagram, the zones include Not Elongate (Class 1), Slightly Elongate (Class 2), Moderately Elongate (Class 3), Very Elongate (Class 4), and Extremely Elongate (Class 5) (Blott and Pye, 2008).

For the Flatness diagram, the zones include Not Flat (Class 1), Slightly Flat (Class 2), Moderately Flat (Class 3), Very Flat (Class 4), and Extremely Flat (Class 5) (Blott and Pye, 2008).

For the Particle Form diagram, it is separated into two versions depending on the roundness of the particles. For angular particles, the zones are plate, slab,

flat block, equant block, sub-equant block, blade, elongate block, and rod. For the round particles, the zones are discoid, very oblate spheroid, oblate spheroid, equant spheroid, sub-equant spheroid, blade, prolate spheroid, and roller (Blott and Pye, 2008).

Flatness Index (FI) and Distance from Source

The flatness index (FI) of a grain is defined using the following formula:

$$FI = (L + W)/(2T) \qquad \text{[Equation 2]}$$

In this formula, L is the length or the longest axis of the grain, W is the width or middle axis, and T is the thickness or shortest axis of the grain (Hérail et. al., 1990). The FI is then used to measure the distance from its source the grain was collected from using the following formula (Cailleux and Tricart, 1959; Hérail et. al., 1990):

$$\text{Distance (km)} = 1.2833 + (FI - 0.57662) + (FI^2 \times 0.31718) \qquad \text{[Equation 3]}$$

CHAPTER SIX:

RESULTS

In March 2018, I witnessed the opening and examination of the contents of Poke 1. The weight of the poke and its contents was 1377.82 g (Figures 12 and 13). Using an ASTM E11 standardized test sieve, the contents were separated into the following weights: <4mm at 347.96g, 2-4 mm at 408.48g, 0.25-2 mm at 612.45g, 0.125-0.25 mm at 8.12g, and pan dust (i.e, <0.125mm) at 1.13g. It should be noted that ASTM sieving procedures were not followed. Due to time constraints and laboratory conditions, this was the only time available to collect this data and the methodology used represents a potential source of minor error.

Figure 12. Showing the contents of Poke 1. At the very bottom of the Poke, a 3-ounce gold slug was found.

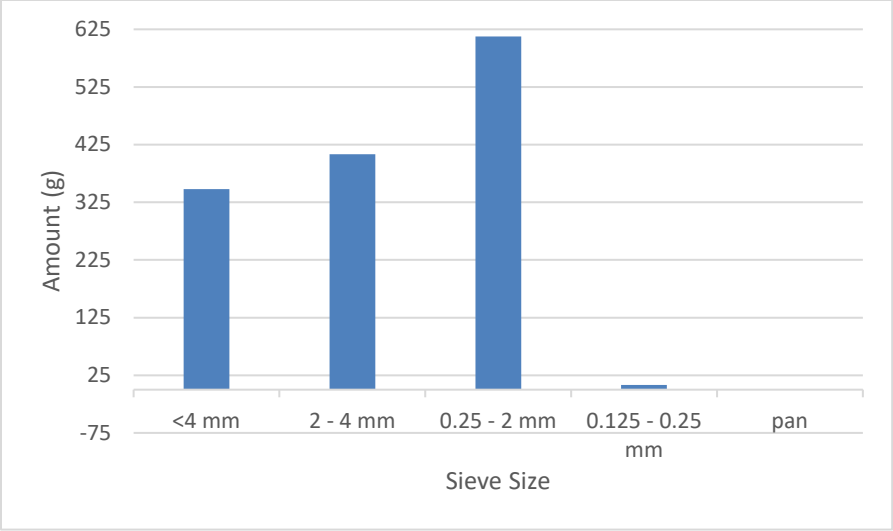

Figure 13. A histogram showing the distribution of grain sizes of the placer gold recovered from Poke 1.

On June 30th, 2018, my advisor, Dr. Erik Melchiorre, returned to Bob's lab to obtain samples from Pokes 2 and 3.

Gold Purity

For gold purity, I plotted my findings on ternary diagrams. Unlike a traditional line graph with two end members, ternary diagrams are used in mineralogy to describe mineral groups with three end members. For native gold, there will always be some combination of gold (Au), silver (Ag), and copper (Cu). Because Cu is usually found in such small quantities, I multiplied its values by 10 to normalize the data (and make it more readable on the graph). Purity data from all Pokes can be found in Appendix C.

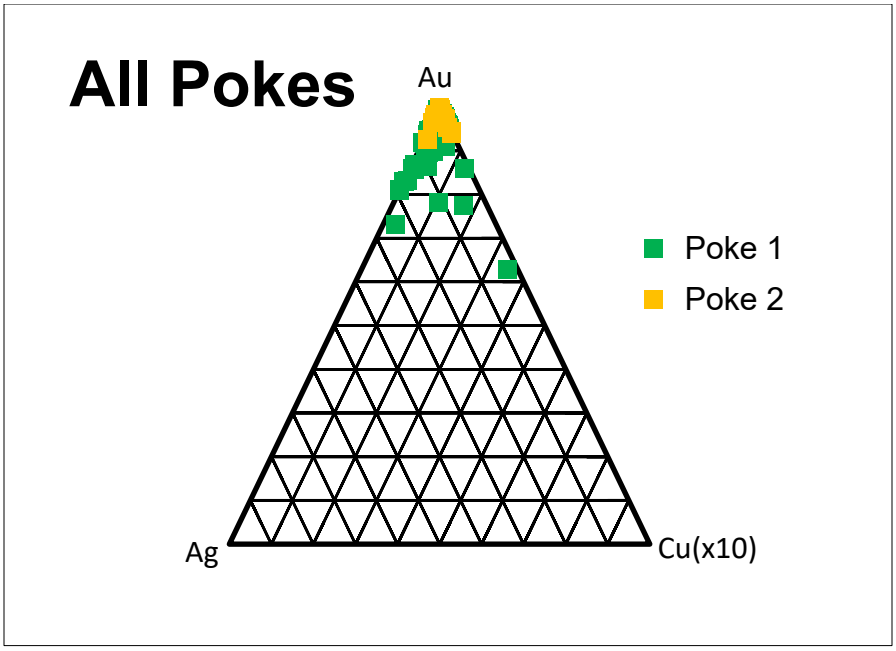

Figure 14. Gold purity data from surface analysis of placer gold nuggets recovered from the SS Central America. Poke 1 is shown in green and Poke 2 is shown in yellow.

Surface analysis data from Pokes 1 and 2 (Figure 14) reveal the gold from the two Pokes have two distinct average purities. Poke 2 (yellow) has a higher gold purity than Poke 1 (green). This suggests that Poke 2 gold either: 1) came from a deposit consisting of a higher purity or 2) was subjected to higher rate of weathering giving the appearance of higher gold purity. Due to restrictions in place from the COVID-19 lockdown, I was unable to collect gold purity data of nuggets from Poke 3.

For Figures 15 and 16, the green squares represent Poke 1, Poke 2 is represented by the yellow squares, and Pokes 3 by the blue squares.

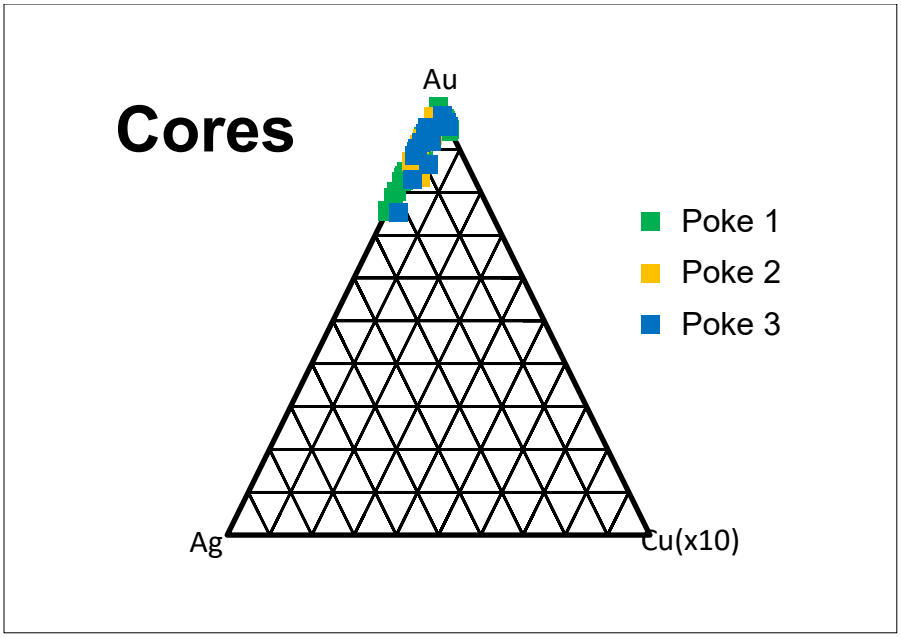

Figure 15. Gold purity core data of placer gold recovered from the SS Central America.

Analysis of core data from all three pokes (Figure 15) showed that most of the gold cores contained higher amounts of Ag than Cu.

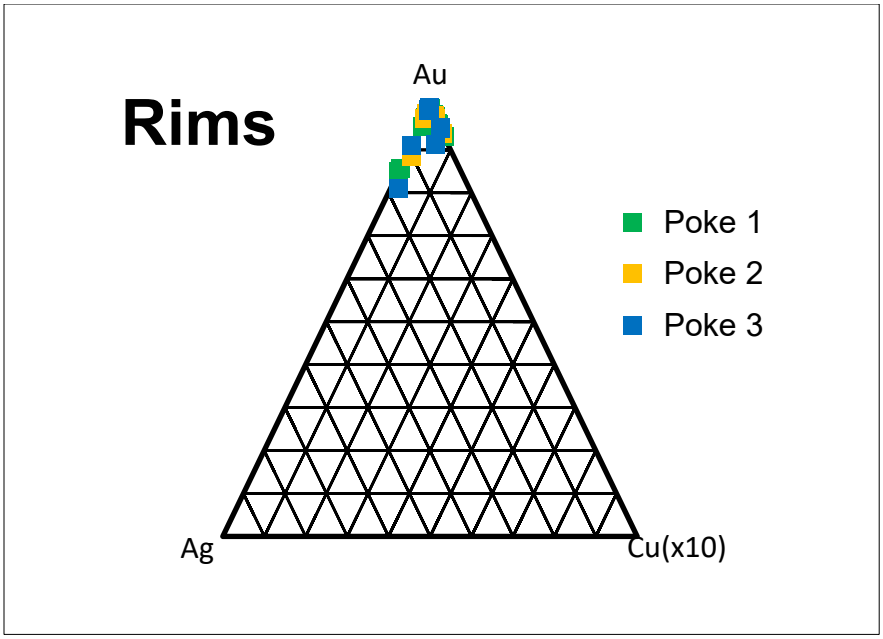

Figure 16. Gold purity rim data of placer gold recovered from the SS Central America.

Analysis of the rim data from placer gold recovered from all three pokes (Figure 16) shows a higher overall concentration of Cu than Ag.

Right away, we notice that the gold purity is higher in the rims than the cores; we expected this. The outside (or rim) of the gold is exposed to weathering processes. These processes remove “impurities” from the gold, giving the illusion of “more gold” atoms, and increases the gold’s purity.

Summary

Poke 1

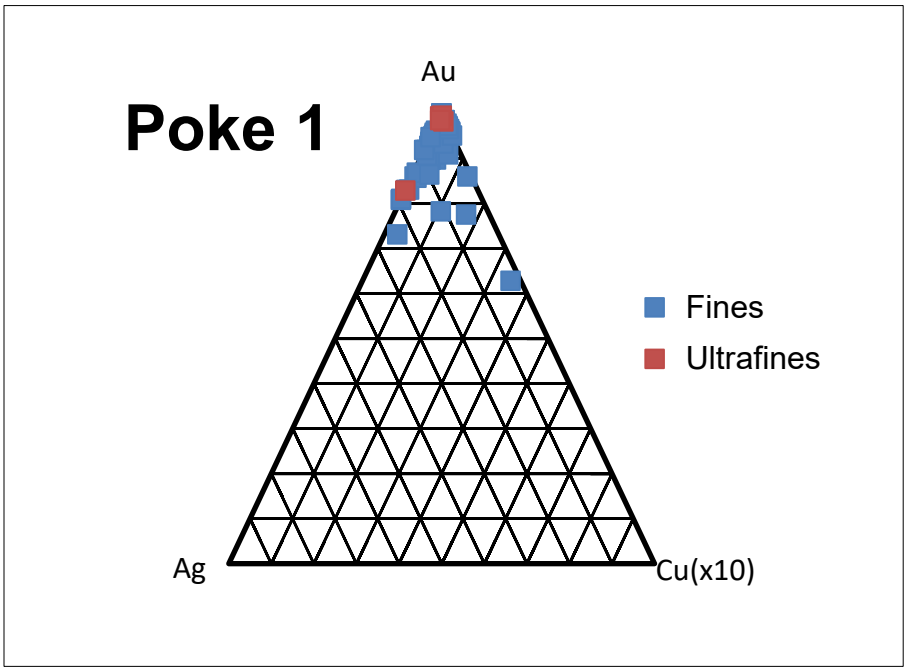

Figure 17. Showing gold purity of placer gold samples recovered from Poke 1.

Surface analysis of fine and ultrafine placer gold recovered from Poke 1 (Figure 17) revealed an overall average purity of 90.80%. For fines, gold purity ranged from 62.82% to 99.99% and had an average purity of 90.29%. For ultrafines, gold purity ranged from 82.89% to 99.52% and averaged at 95.70%. Both fines and ultrafines contained a higher concentration of Ag than Cu.

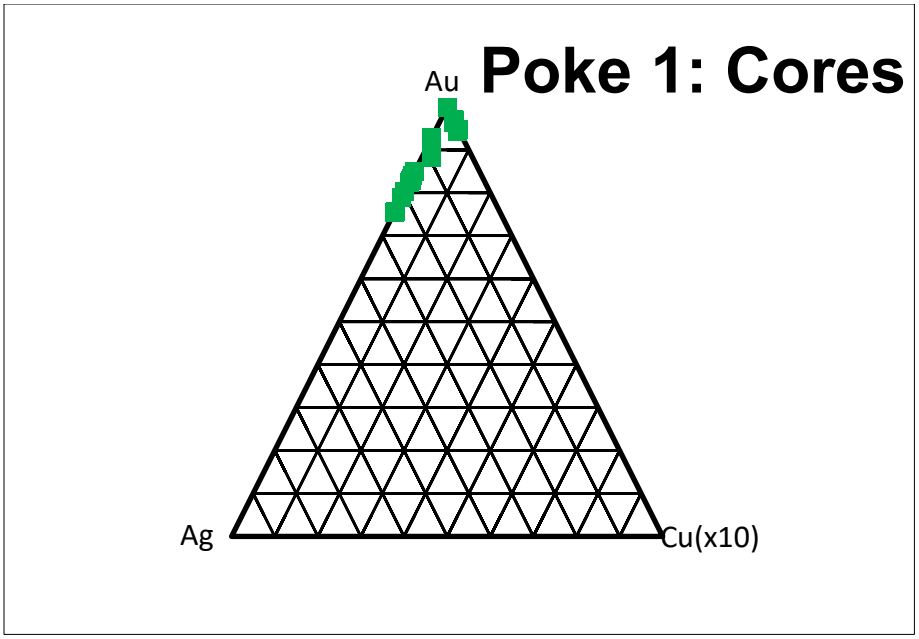

Figure 18. Gold purity core data of placer gold recovered from the Poke 1. The average core purity is 87.41%.

Cores data from Poke 1 showed a purity that ranged from 75.44% to 97.17% and had an average purity of 86.49%. Core data showed a significantly higher concentration of Ag over Cu (Figure 18).

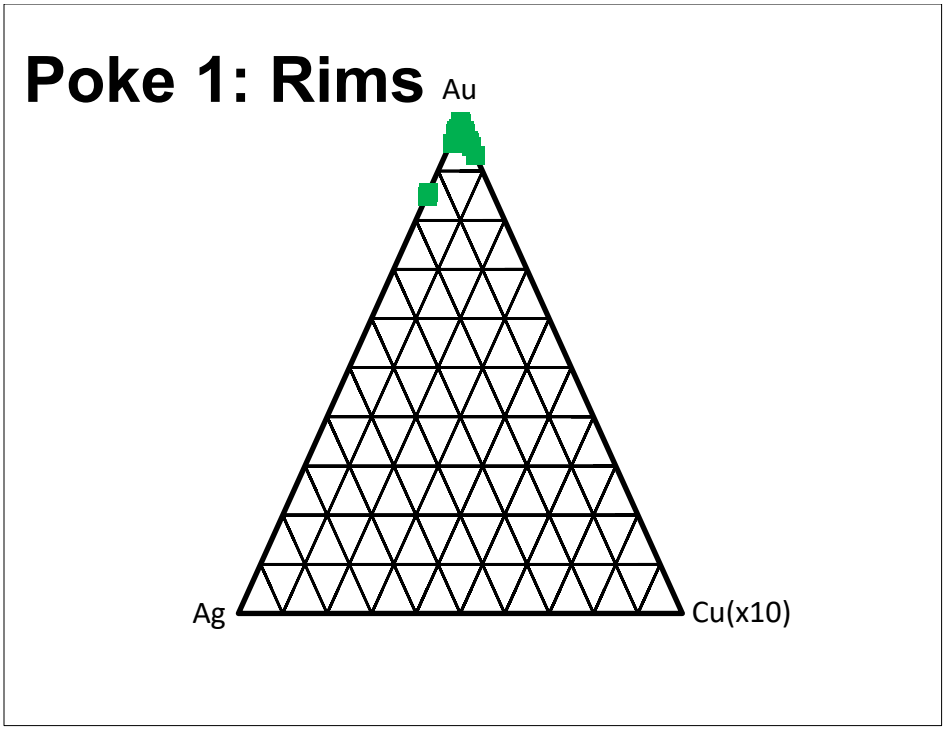

Figure 19. Gold purity rim data of placer gold recovered from the Poke 1. The average rim purity is 95.83%.

Analysis of rim data from Poke 1 showed a range of gold purity from 84.88% to 99.58% and had an average purity of 95.33%. Rim data revealed a higher concentration of Cu than Ag; however, the still is a significant amount of Ag present (Figure 19).

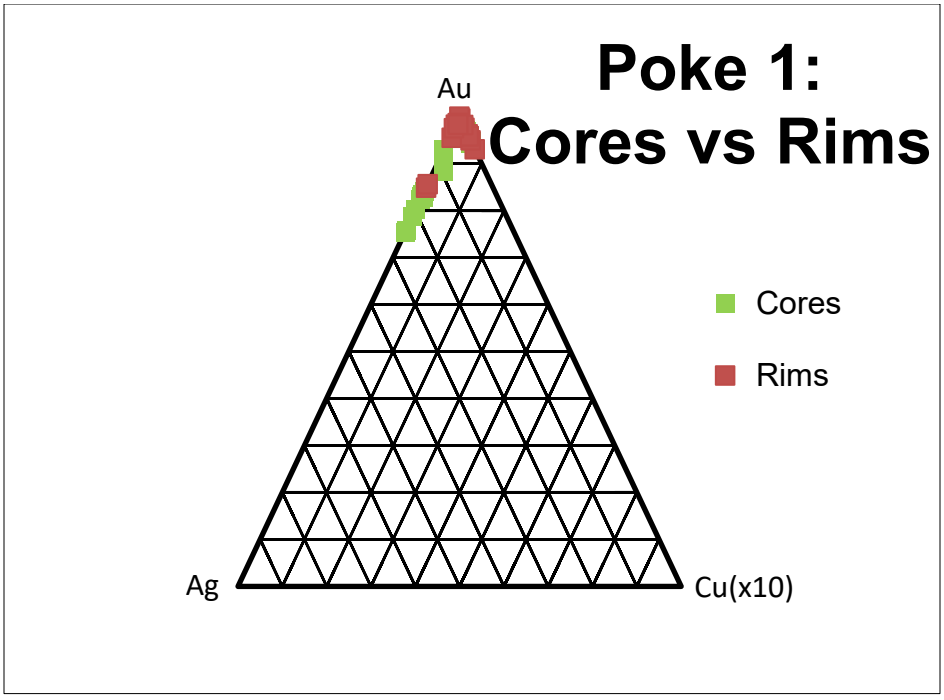

Figure 20. Showing comparison of cores and rims from Poke 1.

Comparison of core and rim data from Poke 1 revealed a higher gold purity for rims (Figure 20). This is due to the fact that the surface of gold is more exposed to weathering processes than the core, or inside, of the gold. Weathering processes breakdown the gold on a molecular level and remove any impurities from the gold structure. The remaining, unaffected gold molecules give the illusion of a more pure gold nugget.

Poke 2

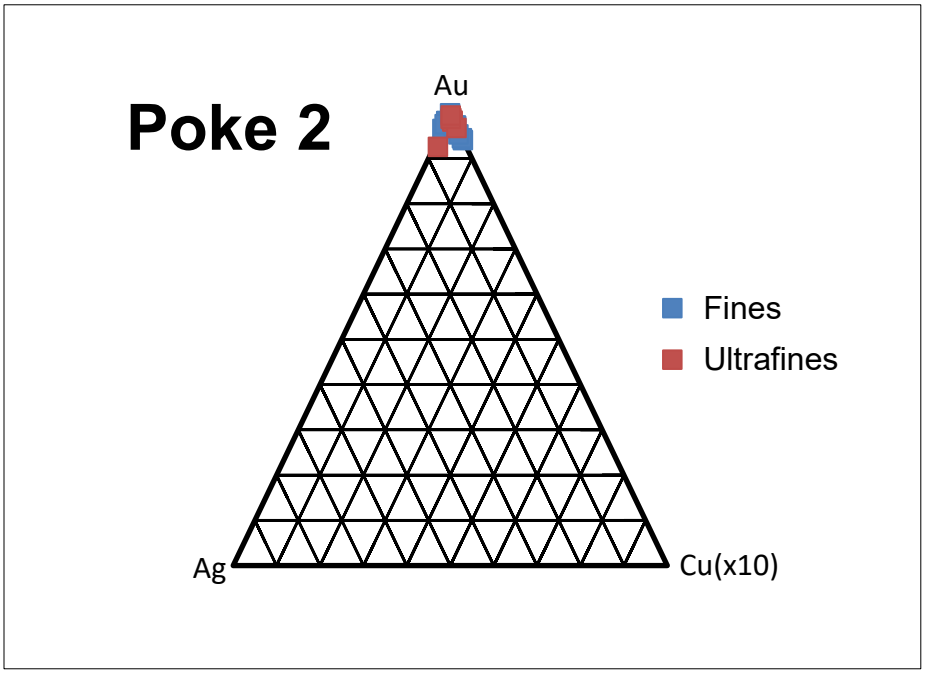

Figure 21. Showing gold purity of placer gold samples recovered from Poke 2. The average purity of placer gold from Poke 2 was %.

Shown in Figure 21, surface data from Poke 2 revealed an overall purity average of 96.11%. For fines, the purity ranged from 79.96% to 98.30% with an average purity of 94.94%. For ultrafines, the purity ranged from 92.56% to 99.47% with an average of 97.72%.

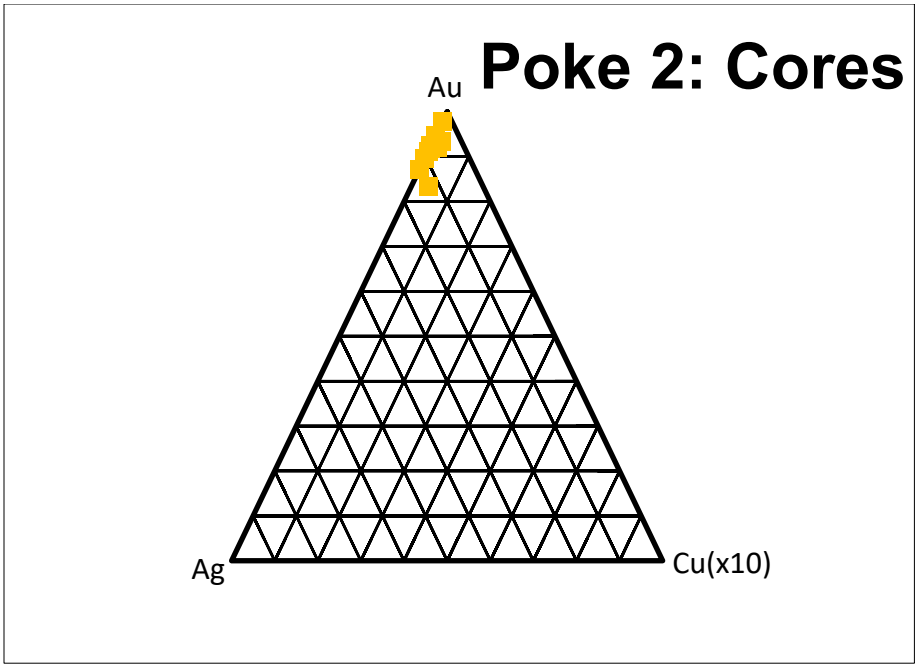

Figure 22. Gold purity core data of placer gold recovered from the Poke 2. The average core purity is %.

Core data from Poke 2 ranged from 83.44% to 97.74% and averaged at 91.49%. Analysis revealed a significantly higher concentration of Ag and minimal amounts of Cu (Figure 22).

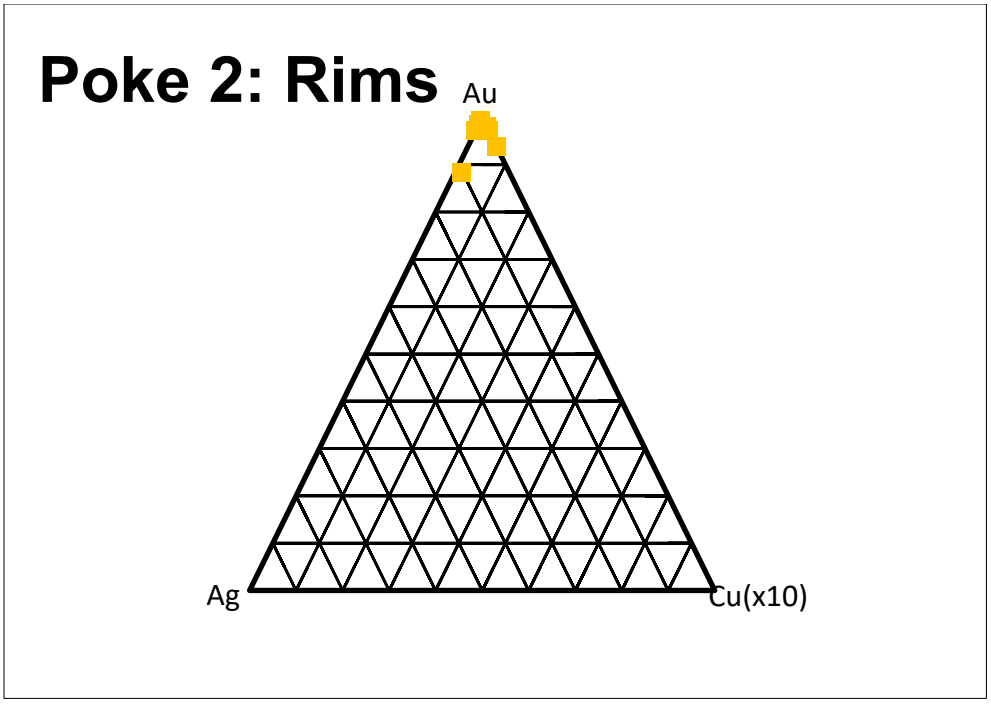

Figure 23. Gold purity rim data of placer gold recovered from the Poke 2. The average rim purity is %.

Analysis of gold purity of rims showed a range of 88.38% to 99.31% and averaged at 96.09%. There was a significant increase in the concentration of Cu, as well as, some Ag (Figure 23).

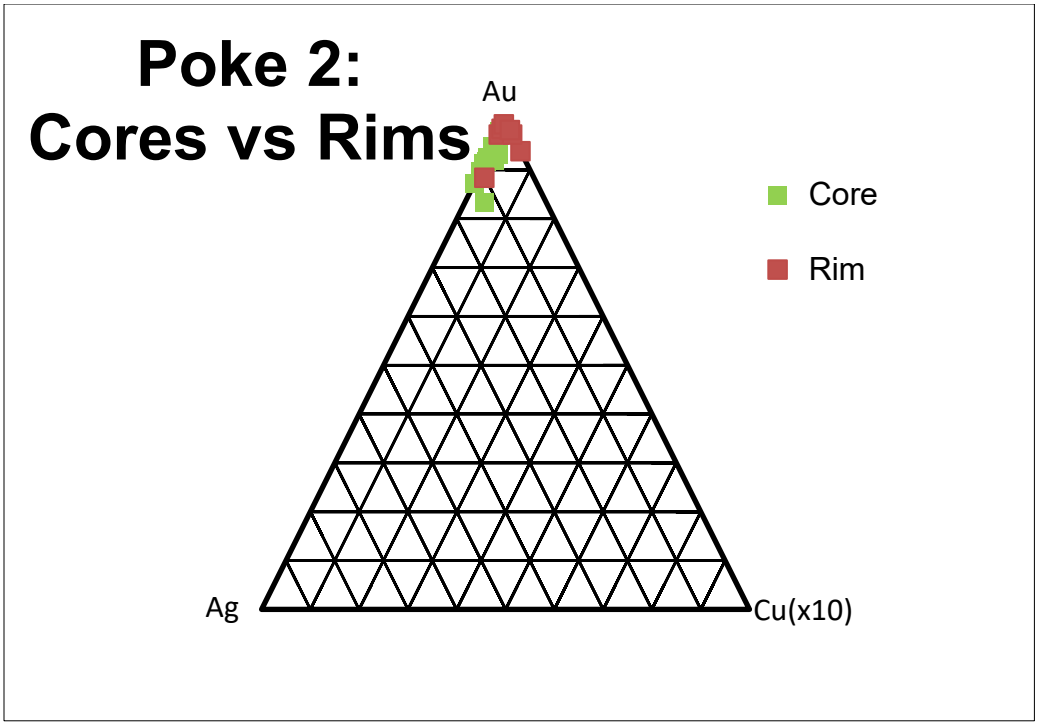

Figure 24. Showing comparison of cores and rims from Poke 2.

Comparison of core and rim data from Poke 2 revealed the rims had a higher gold purity (Figure 24).

Poke 3

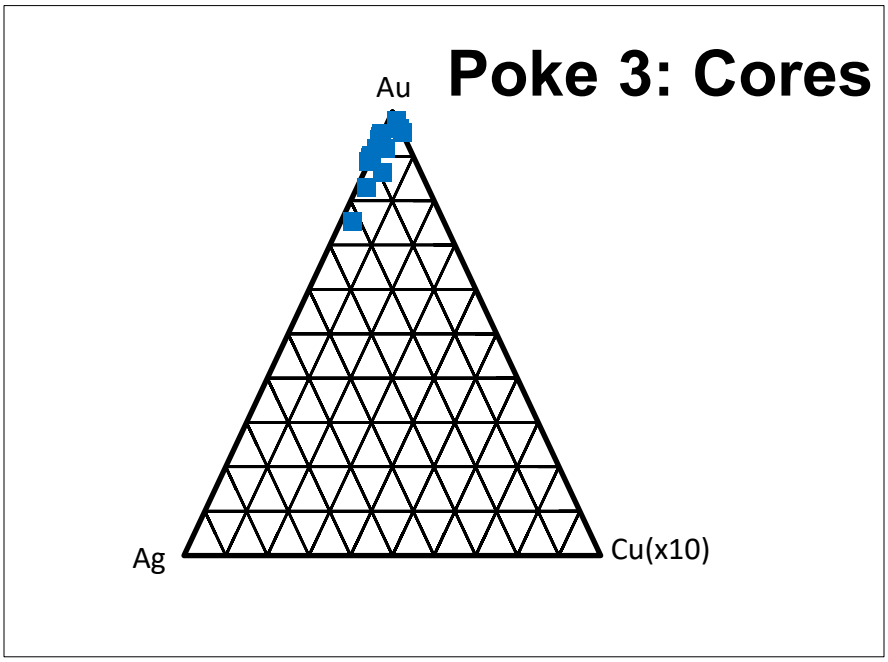

Figure 25. Gold purity core data of placer gold recovered from the Poke 3. The average core purity is 90.65%.

Core purity data from Poke 3 showed a range from 75.37% to 98.04% and averaged 90.65%. There was significantly more Ag than Cu found in the cores (Figure 25).

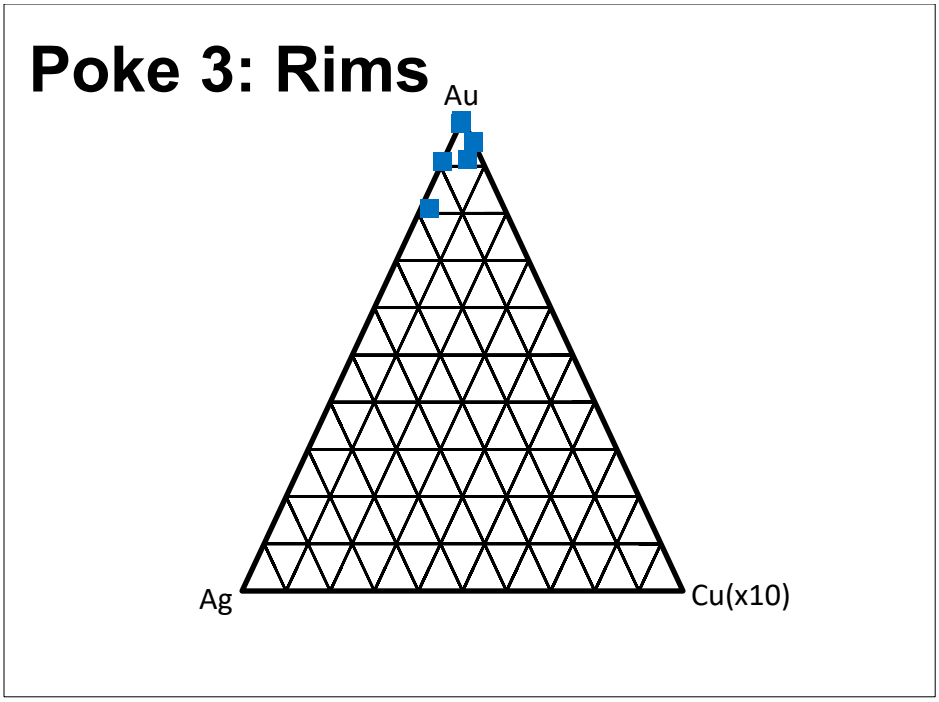

Figure 26. Gold purity rim data of placer gold recovered from the Poke 3. The average rim purity is 94.61%.

Analysis of rim purity from Poke 3 ranged from 81.09% to 99.73% and averaged 94.61% (Figure 26).

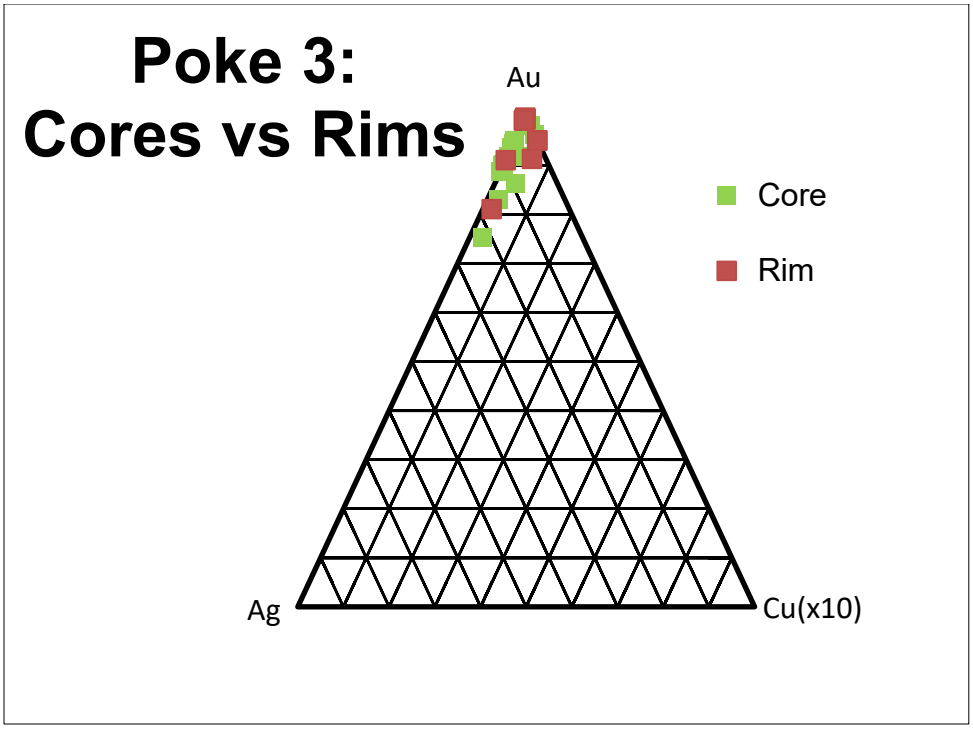

Figure 27. Showing comparison of cores and rims from Poke 3.

Comparison of core and rim data from Poke 3 (Figure 27) revealed that, although the rims had a higher purity average, both the cores and rims showed purities above 90%.

Inclusions

Summary

For gold from Poke 3, Figure 28 shows an inclusion with a high silicon (Si) content. Further analysis of the grain revealed concentrations of sodium (Na), oxygen (O), and aluminum (Al) suggesting that this is a member of the feldspar

group. The abundance of Na further indicates this an albite crystal. The feldspar group is the second most abundant mineral group in the earth's crust (behind the quartz group).

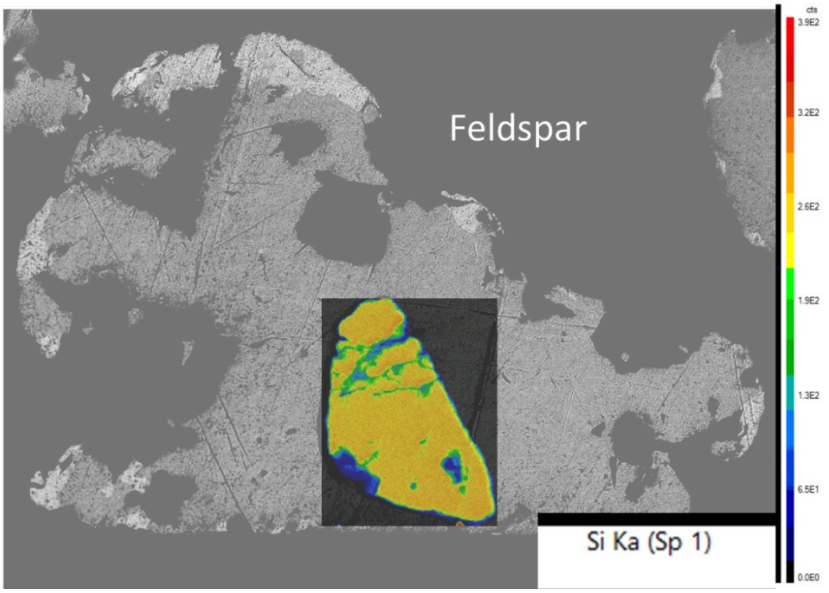

Figure 28. Showing a Feldspar inclusion from Poke 3. The greyscale photo is a backscatter image, with brightness reflecting denser elements. The color inset exactly superimposes on the backscatter image to show the distribution of silicon within the inclusion. Similar maps of intensity for aluminum and sodium and their relative elemental abundance suggest this is an albite inclusion.

Figure 29 shows a pyrite crystal with a perfect cubic structure observed in gold from Poke 3. Pyrite (FeS_2) is the most common mineral of the sulfide group. Pyrite is more commonly known as "Fool's Gold."

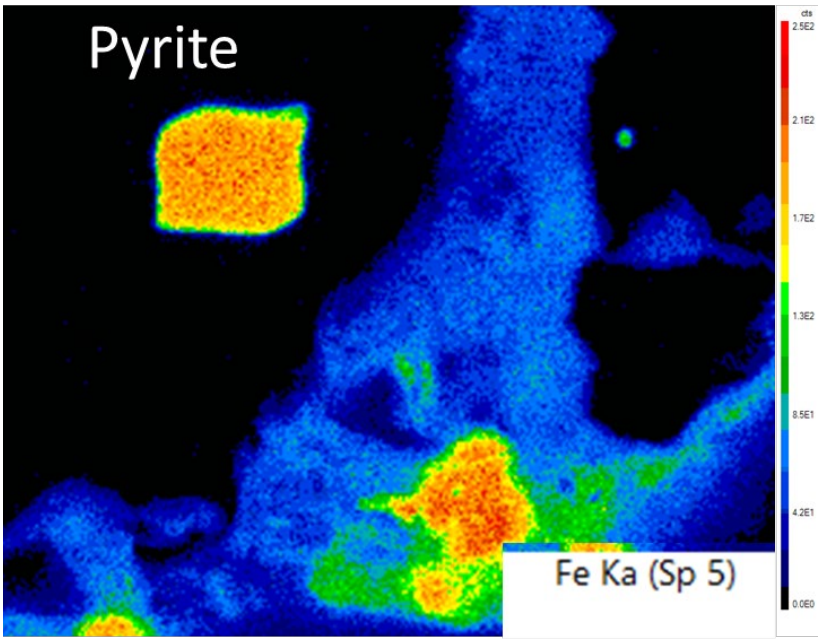

Figure 29. Showing a pyrite inclusion observed in Poke 3. This EDS map of the abundance of iron shows relative abundances from low (dark blue) to high (progressively warmer colors). A similar distribution map for sulfur suggests this is a pyrite cube. Below it, the red zone with a surrounding halo of green is diffuse iron oxide minerals that probably result from the weathering dissolution of a similar but more exposed pyrite crystal.

In Figure 30, spots 1, 3, 4, and 5 show inclusions that had concentrations of lead (Pb), oxygen (O), and sulfur (S) in the gold from Poke 2. The presence of S and O suggests this is a sulfate mineral. The presence of Pb further suggests this is the rare lead sulfate mineral, anglesite ($PbSO_4$), which forms as the most common oxidation product of galena, a major ore of Pb.

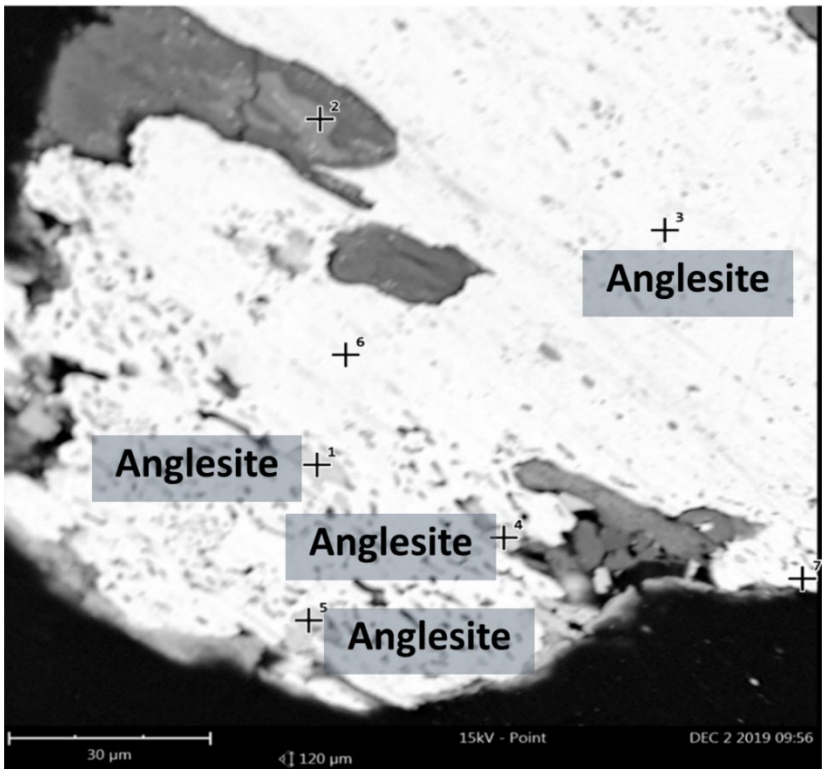

Figure 30. Backscatter electron image showing light grey anglesite inclusions in bright white gold from Poke 2. Increasing brightness indicates denser elements. The dark grey inclusions are unidentified iron oxides with a low concentration of lead.

A full breakdown of the inclusion data can be found in Appendix D.

Poke 1

Minerals that were identified as inclusions in Poke 1 gold include native iridium, albite, fayalite, Ni-bearing pyrrhotite, augite, galena, and rutile. Other minerals of lower abundance include wulfenite, anadite, phlogopite, cerrusite, cotunnite, andalusite, kyanite, sillimanite, anatase, brookite, and cordierite.

Poke 2

Minerals that were identified as inclusions in Poke 2 gold include anglesite, chalcopyrite, and albite. Other minerals with weaker certainty of identificaton include fayalite and anandite, a rare sulfur-bearing mica.

Poke 3

The minerals identified as inclusions in Poke 3 gold were pyrite and albite. Other possible minerals include quartz, cordierite, and star garnet, a variety of almandine often found with rutile.

Accessory Minerals

Summary

Some minerals are prevalent and can be found in almost any waterway on earth. An example of this would be quartz, the most abundant mineral in the earth's crust. Figure 31 shows a perfectly shaped quartz crystal. Notice that the image is showing silicon (Si) concentrations. Other common minerals I found include pyrite, magnetite, ilmenite, and rutile.

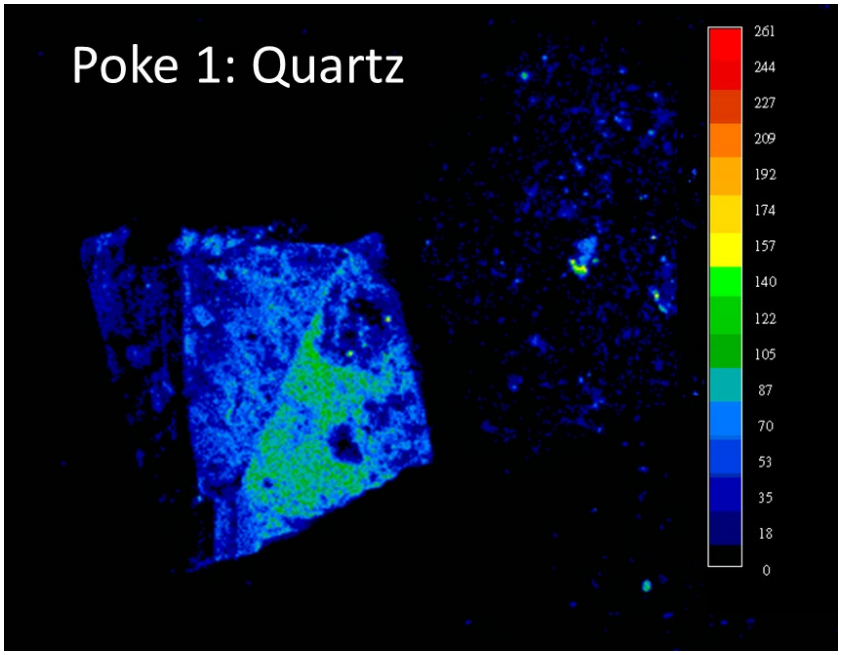

Figure 31. Elemental mapping of silicon abundance reveals a perfect quartz crystal. Lower apparent silicon intensity is caused by a coating of iron oxide from the shipwreck iron.

Other minerals are less common and can only be found in specific waterways. An example of this would be palladium, a native element that is part of the Platinum Group Metals (PGMs). PGMs are quite rare, with the crustal abundance of palladium being 1.5 x 10^-3 or (0.0015) ppm, which is significantly less than gold (Helmenstine, 2018). Figure 32 shows a perfect palladium crystal observed in Poke 1; notice this image is showing Pd concentrations. Because the palladium is found in a placer deposit, it is most likely that it and the gold (which come from gold-quartz veins) were weathered out of different veins that eroded into the same waterway. In the Sierra Nevada foothills, metals such as palladium

are usually associated with serpentinite veins (Sjoberg and Gomes, 1981). Future investigations should look at the relationship between platinum group metals and gold placer deposits in California.

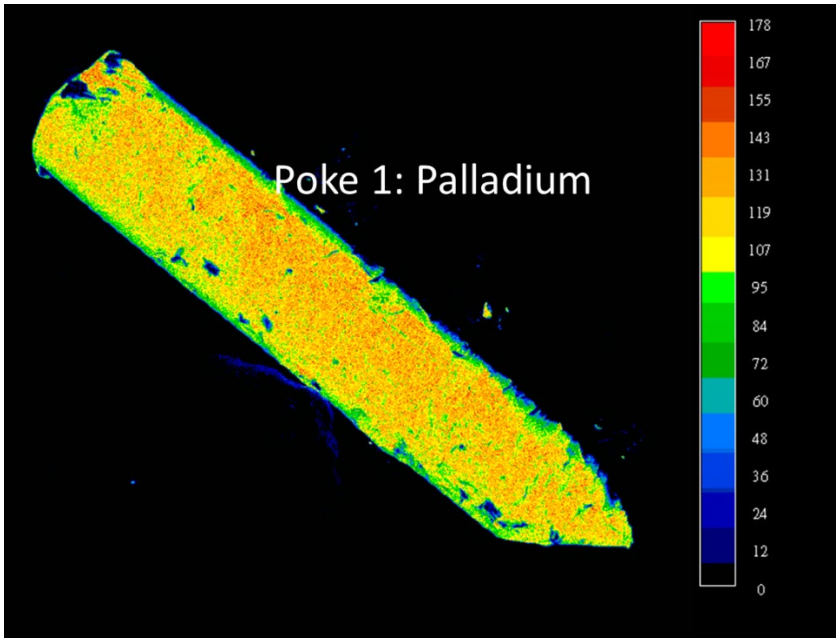

Figure 32. Elemental map for palladium abundance, revealing an elongated single palladium crystal. Sample is from Poke 1.

Poke 1

The identified accessory minerals from Poke 1 include palladium, pyrite, hematite, zircon, magnetite, and ilmenite. Other possible minerals include pabstite, titanite, bornite, idaite, cubanite, and chalcopyrite.

Poke 2

The only accessory mineral identified in black sands from Poke 2 was an albite crystal with interstitial augite (Figure 33 and Table 15).

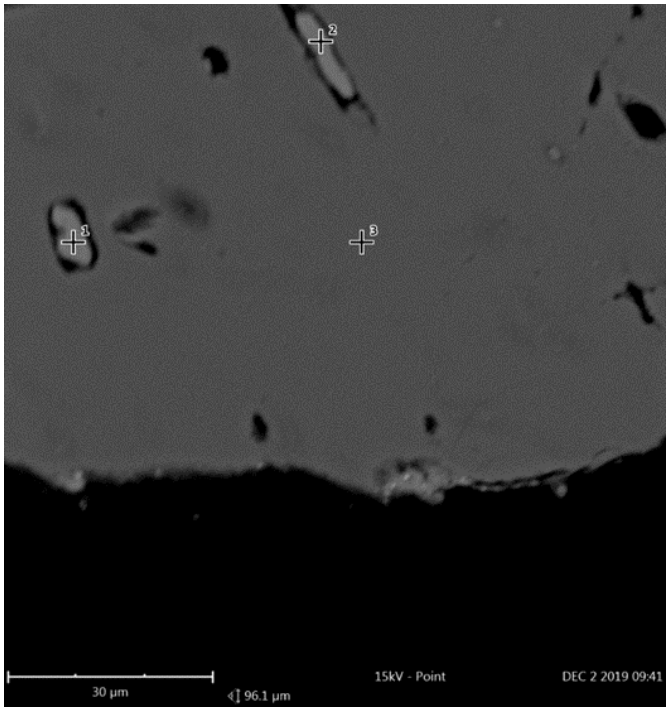

Figure 33. Showing albite crystal (point 3) with interstitial augite (points 1 and 2).

Poke 3

No accessory minerals were identified from Poke 3 due to restrictions in place from the COVID-19 lockdown. Future work will be needed to compile a list of accessory minerals for Poke 3.

Morphology

Summary

Due to campus closure due to the COVID-19 outbreak and state ‘stay-at-home’ orders, I was unable to access the lab to finish collecting morphological data; however, the data presented here was collected prior to lockdown. A full breakdown of the morphology data can be found in Appendix F.

Poke 1

The morphology of grains analyzed in Poke 1 (Table 16) plotted mainly on the “disc” and “blade” zones on the Zingg diagram (Figure 34). These included all the fines from groups 1 and 2, as well as the 4mm and 2-4mm rounded particles. Some 4mm and 2-4mm crystals also plotted in these fields. The rest of the 4mm and 2-4mm crystals plotted in the “sphere” and “rod” zones of the Zingg diagram.

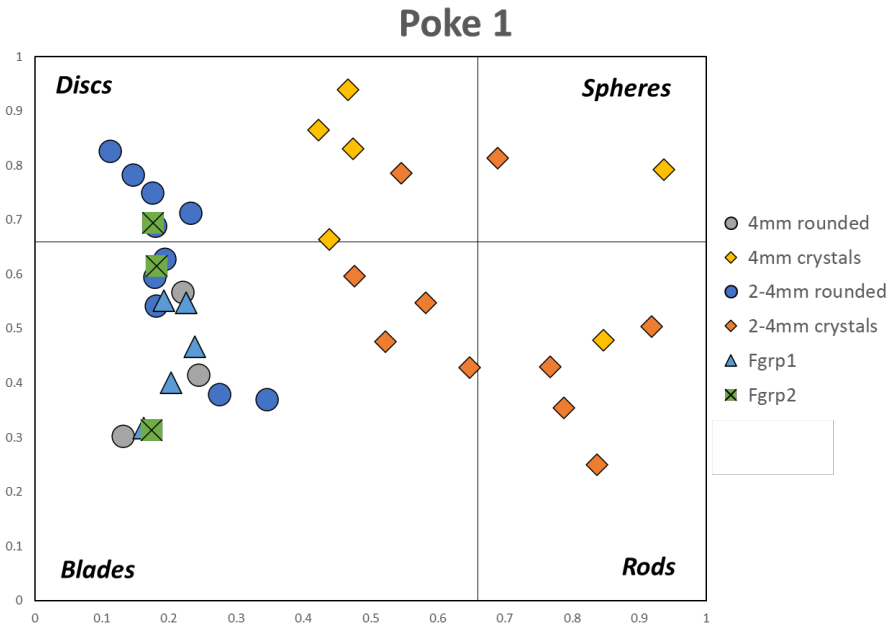

Figure 34. Traditional Zingg Diagram showing analysis of grains from Poke 1. The axes are defined as Thickness/Width (T/W) and Width/Length (W/L).

The same grains from Poke 1 were plotted on an Elongation diagram (Figure 35). The 4mm rounded grains plotted in Classes 3 and 4. The 4mm crystal grains plotted in Classes 1, 2, and 3. The 2-4mm rounded and crystal grains plotted in Classes 1, 2, 3, and 4. The fines from group 1 plotted in Classes 3 and 4. The fines from group 2 plotted in Class 2 and 4.

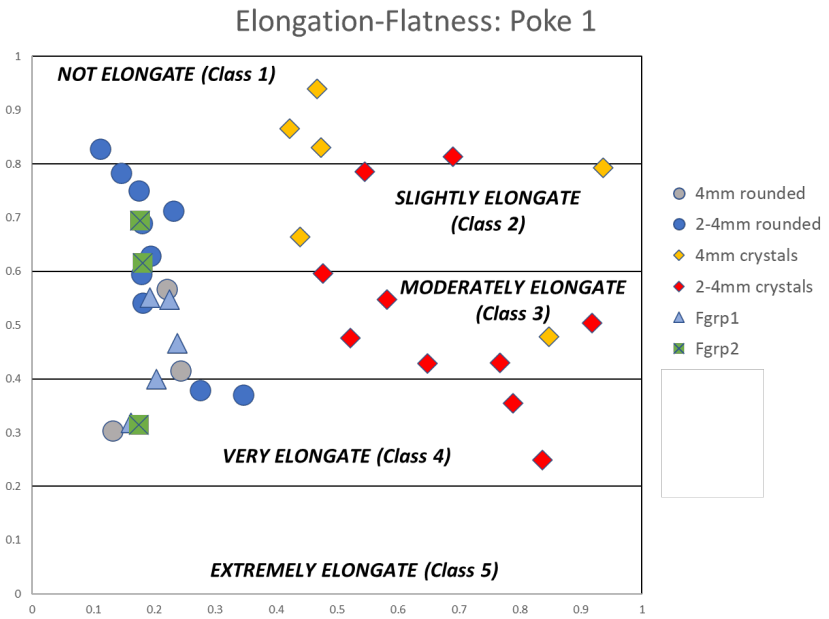

Figure 35. Showing the Elongation diagram for Poke 1.

The grains from Poke 1 were also plotted on a Flatness diagram (Figure 36). The 4mm and 2-4mm rounded grains plotted in Classes 4 and 5. The 4mm and 2-4mm crystal grains plotted in Classes 1, 2, and 3. The fines from group 1 plotted in Classes 4 and 5. The fines from group 2 all plotted in Class 5.

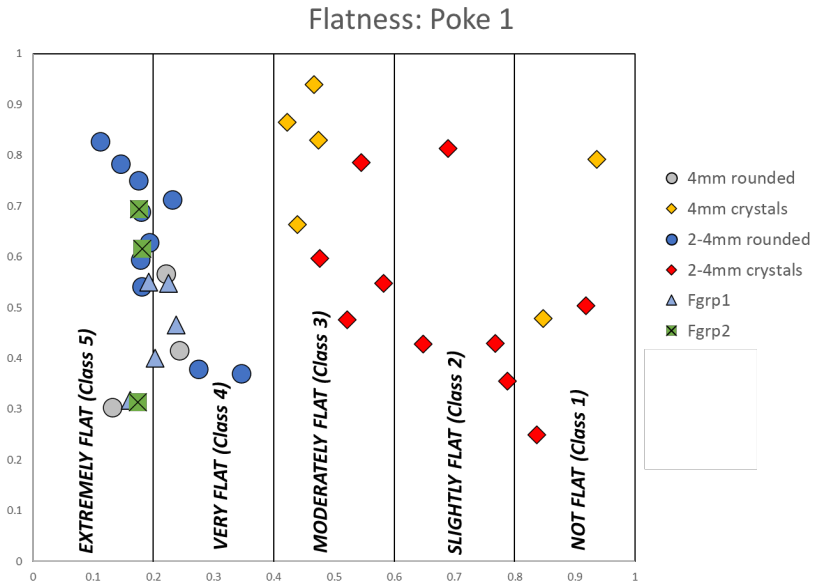

Figure 36. Showing the Flatness diagram for Poke 1.

Finally, the grains from Poke 1 were plotted on a Particle Form diagram (Figure 37). All the 4mm rounded grains plotted in the “blade” zone. The 4mm crystal grains plotted in the “flat block”, “elongate block”, and “sub-equant block” zones. The 2-4mm rounded grains plotted in the “discoid”, “very oblate spheroid”, and “blade” zones. The 2-4mm crystal grains plotted in the “flat block”, “sub-equant block”, “blade”, “elongate block”, and “rod” zones. All the fines from group 1 plotted in the “blade” zone and the fines from group 2 plotted in the “plate/discoid” and “blade” zones.

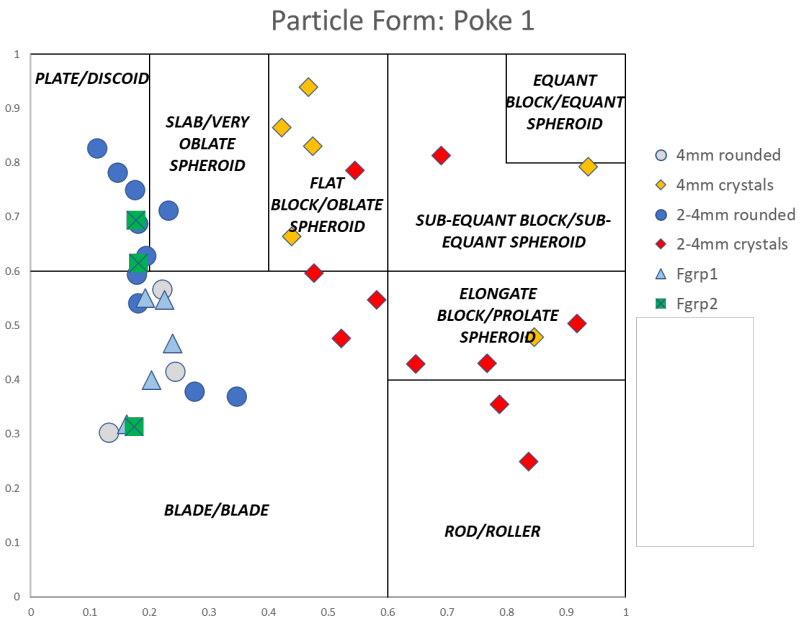

Figure 37. Showing Particle Form data from Poke 1.

The flatness index (FI) and distance from source data for nuggets from Poke 1 (Table 16) were plotted on a FI vs Distance diagram (Figure 38). The rounded grains had FIs between 4.5 and 11 and were collected from 5 – 30 km from their source. The crystalline grains had FIs between 1 and 3 and were collected less than 5 km from their source rock.

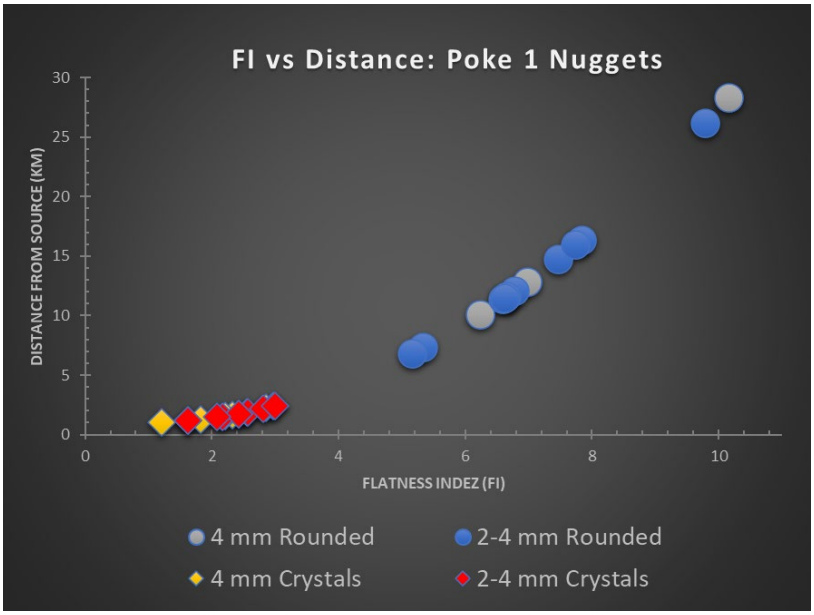

Figure 38. Showing a comparison of all 4mm and 2-4mm grains analyzed from Poke 1. We see two clear species, crystalline nuggets (in yellow and red) and rounded nuggets (in blue and gray).

The FI and distance data for the fines from Poke 1 (Table 16) were also plotted (Figure 39). The fines had FIs between 6 and 10 and were collected 9 to 25 km from their source rock.

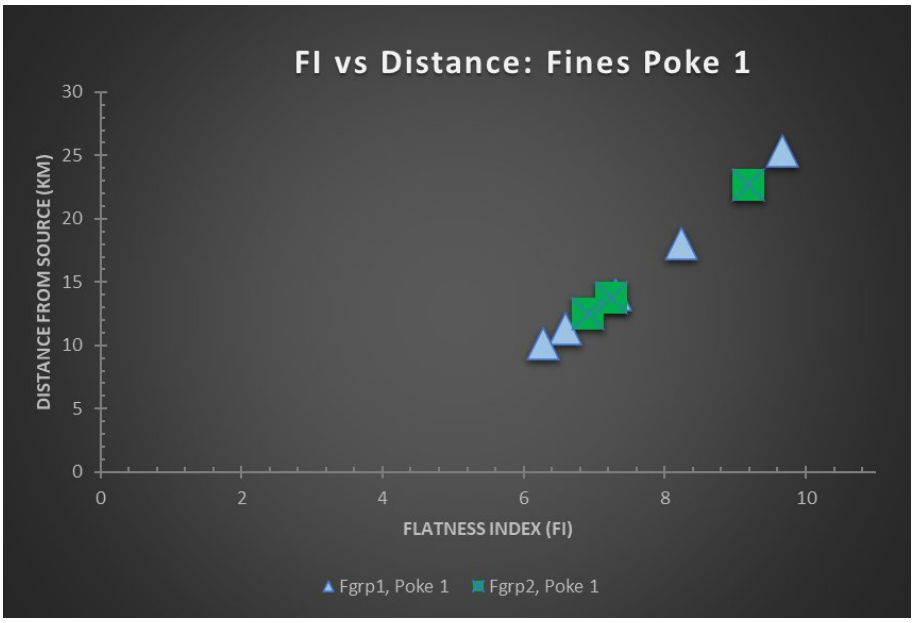

Figure 39 shows a comparison of fines from Poke 1 (light blue triangles and green X's). It appears that the finer gold from Poke 1 was collected farther from its source as the grains have a higher flatness index.

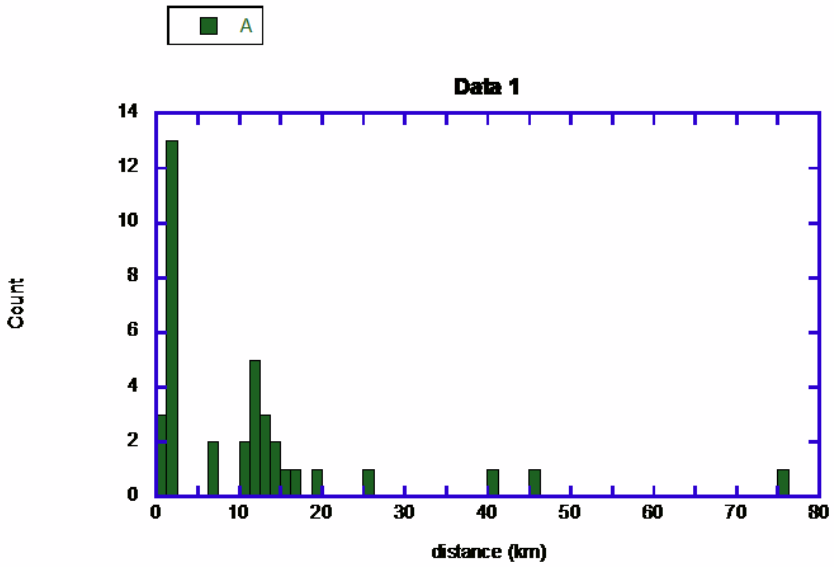

Figure 40. Showing a histogram of the distances grains from Poke 1 were collected from their sources using FI data (Source: Melchiorre, 2021).

Poke 2

The morphology data of ultrafine grains from Poke 2 (Table 17) only plotted in the “blade” and “rod” zones of the Zingg diagram (Figure 41).

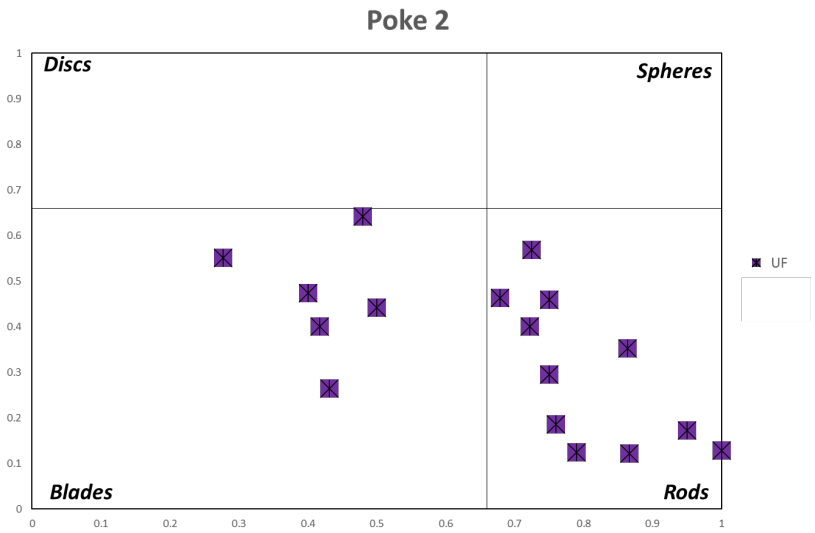

Figure 41. Showing Zingg diagram for Poke 2.

The ultrafine grains from Poke 2 were also plotted on a Elongation diagram; they plotted in Classes 2, 3, 4, and 5 (Figure 42). There were no plots in Class 1.

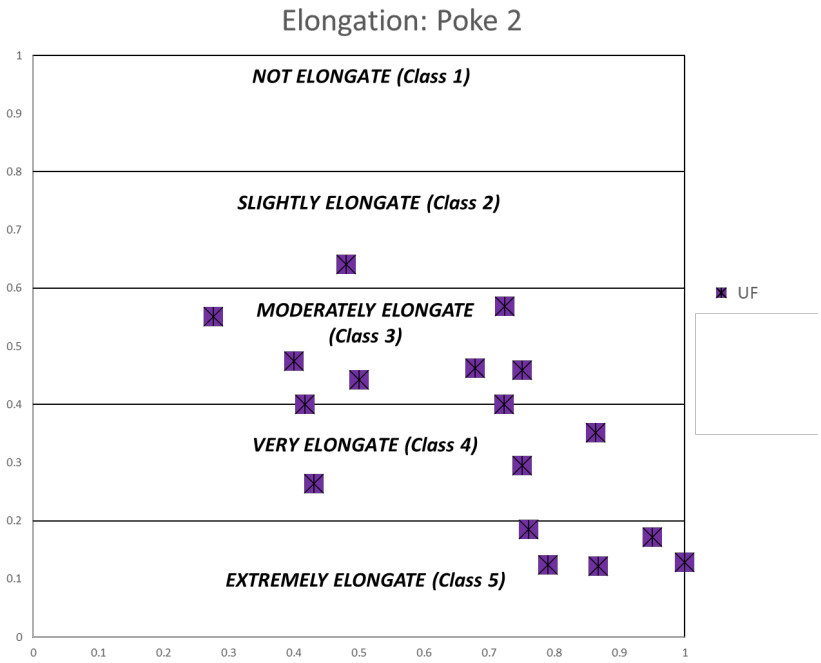

Figure 42. Showing Elongation diagram for Poke 2.

Ultrafine data from Poke 2 was also plotted on a Flatness diagram (Figure 43). The ultrafines from Poke 2 plotted in Classes 1, 2, 3, and 4. There were no plots in Class 5.

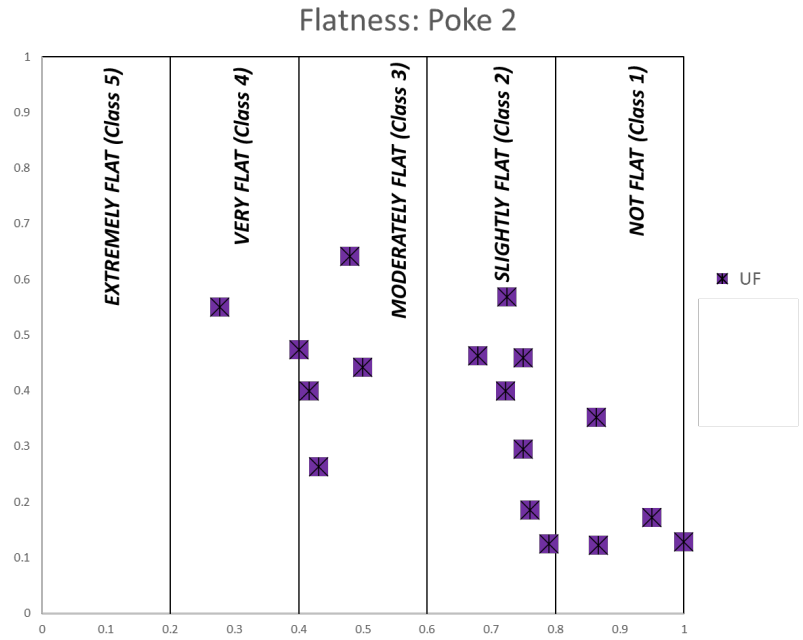

Figure 43. Showing Flatness diagram from Poke 2.

Finally, the ultrafine grains from Poke 2 were plotted on a Particle form diagram (Figure 44). The majority of the grains plotted in the “rod/roller” zone. The rest of the grains plotted in the “blade”, “elongate block/prolate spheroid”, and “flat black/oblate spheroid” zones.

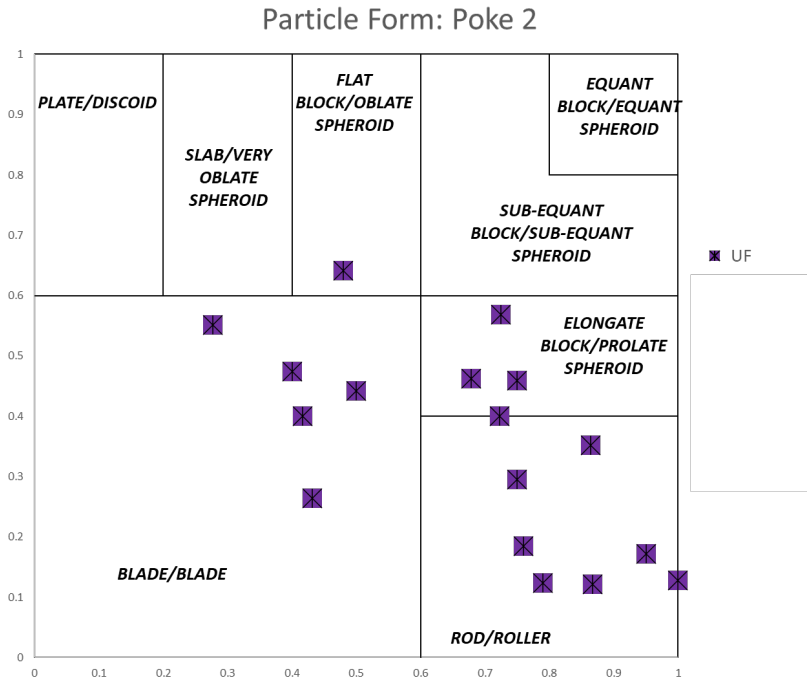

Figure 44. Showing particle form data from Poke 2.

The FI and Distance data (Table 17) plot is shown in Figure 45. There appear to be two species of grains: more rounded grains and less rounded grains. For the more rounded grains, they had FIs between 1 and 5 and were collected 1 to 5 km from their source. For the less rounded grains, they had FIs between 5 and 6 and were collected 6 to 9 km from their source rock.

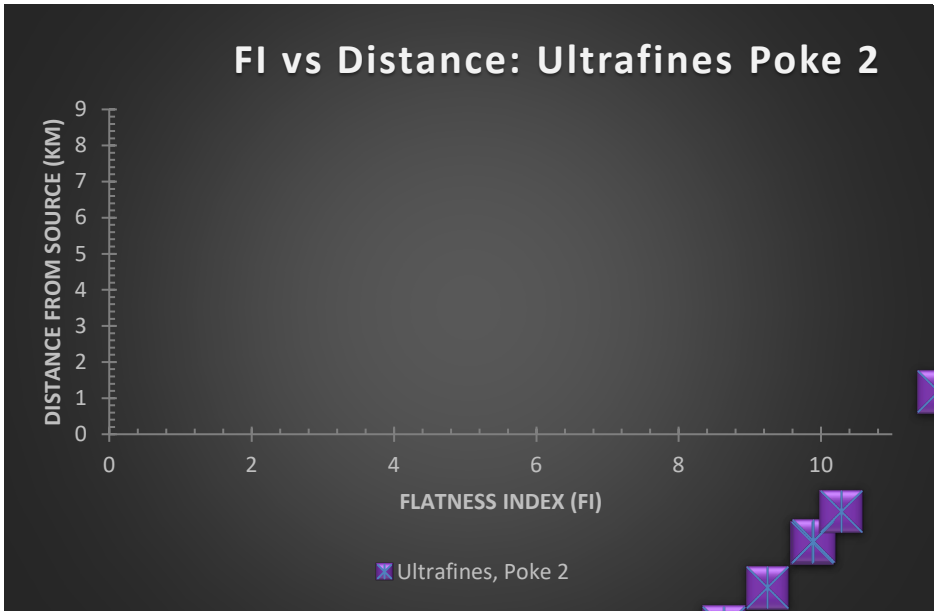

Figure 45. Showing a comparison of ultrafines from Poke 2 (in purple asterisks). Gold from Poke 2 seems to have been collected closer to their source as they have a lower flatness index.

Poke 3

Due to COVID-19 shutting down campus, no morphology data was collected for Poke 3.

CHAPTER SEVEN:

DISCUSSION

Overview

Grain Size Distribution: Poke 1

The grain size distribution shows that this was a sample of gold recovered by a method that was effective down to about 0.25mm. Below that, there was minimal recovery; however, the presence of this finer gold (<0.25 mm) suggests that mercury was not used at the operation. The mix of grain sizes, including a 3 troy ounce nugget, and the presence of black sands, suggest the contents of Poke 1 were the cleanup from a small company's long-tom operation. Processing to remove black sands was minimal, and the distribution of gold particle sizes is likely to closely mirror the distribution in the original source, minus the efficiencies of the recovery method used.

Due to the COVID-19 lockdown, I was not able to collect size data for Poke 2 and Poke 3.

Gold Purity

The overall gold purity of placer gold analyzed from all three pokes is characteristic of the placer gold which was mined from the Mother Lode region of California. Based on their average purities, gold from Poke 1 (average of 90.80%) may have come from the Amador or Butte mining districts, gold from Poke 2 (average of 96.11%) may have been collected from the Yuba mining

district, and gold from Poke 3 (average of 90.65%) may have come from the Amador or Butte mining districts.

The presence of mercury (Hg) on the surface of gold but not in the core of it suggests the Hg is a secondary deposition on the surface from anthropogenic sources (i.e., it did not form with the gold). Large scale mining operations commonly used Hg during the Gold Rush. Therefore, the high accumulations of fugitive Hg on the surface of the gold could only have been found downstream from significant mining operations. Yet the presence of finer grained gold from these pokes indicates that Hg was not directly used during recovery of the gold, but rather occurred due to local contamination by a major mining operation.

Inclusions and Accessory Minerals

Inclusions within the interior of placer gold were formed at the same time as the gold. Their analysis can help further narrow down possible locations the gold was collected from. Although most of the inclusions were of common minerals, there were also some rare minerals. One such example is anglesite, which, in the Mother Lode region of California, is only found along the Upper Feather River. Anglesite inclusions were only found in gold analyzed from Poke 2. Anglesite was identified as inclusions in the placer gold from Poke 2.

Dense accessory minerals, also known as black sands, are commonly collected with the placer gold as it is separated from river sediments during mining operations. Many common minerals can be identified in these black sands; however, there are also some rarer minerals that can be used to

fingerprint specific waterways. One example of a rare mineral found with the gold in Poke 1 is palladium (Pd). In the portions of California's Mother Lode region which were active before 1857, Pd is only reported from the Yuba River.

Morphology

Analysis of the morphology of the placer gold collected from Poke 1 and Poke 2 revealed two specific species: rounded gold and angular gold. Angular gold was collected closer to their original source rock as they had not been battered and original shapes modifies as the ductile gold grains moved down the river system. The rounded gold, on the other hand, was collected farther from its source rock as movement along the river channel completely altered the shape of the gold. The mixture of distinct rounded and angular gold populations within specific pokes indicates either mixing of gold mined from two localities or mining at a locality that contained gold from two distinct sources.

The wide range of the grain sizes in all the gold (i.e., >4mm to 125 microns) suggests that this gold was not collected using Hg amalgamation. Hg amalgamation will absorb flour gold; if this gold had been collected using these techniques, there would be no flour gold present. The morphology of the fine gold mimics the morphology of the coarser gold, which indicates that while mercury was present it was not in quantities sufficient to modify grain shape significantly.

Due to the size distribution of the gold, it is unlikely that "dry washing" methods were used to extract the gold (Table 1). This is because dry washing techniques are not able to recover fined-grained particles (i.e., 40 microns to 2

mm). The placer gold sizes for all pokes recovered from the vest ranged from >4mm to 125 microns.

Possible sources

The morphology and range of particle sizes found in each poke suggests the gold was collected from active stream channels. The shape and size of the gold suggests it was collected by wet treatment gravity concentration mining methods which were commonly employed by small groups of miners during the time of Tertiary gravel mining during the mid-1800s.

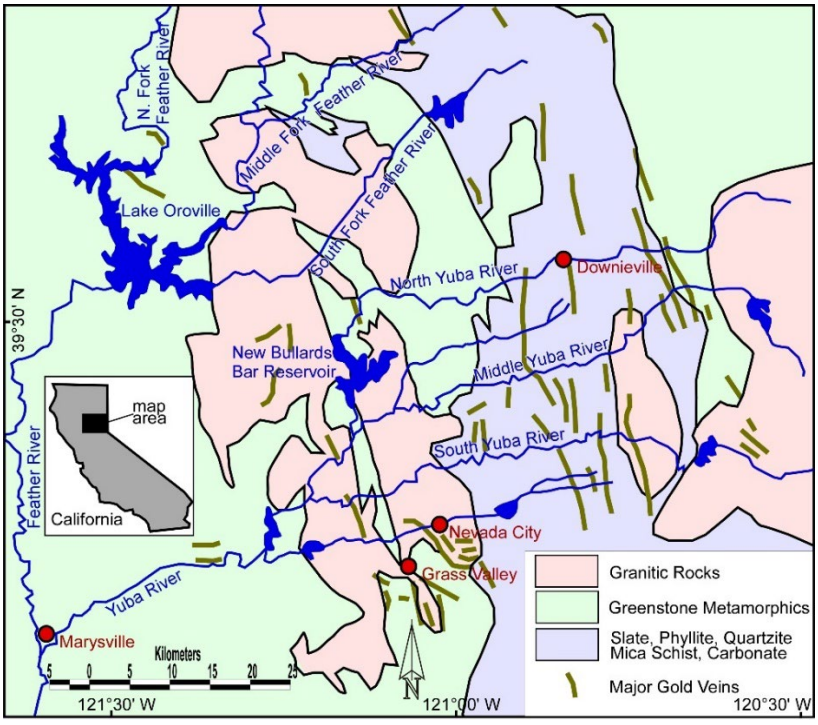

Figure 46. Map showing the locations of the Yuba and Feather Rivers of California and the rock type/s these rivers are situated on (Clark, 1970).

The presences of the rarer minerals suggest the gold from each poke came from two different sources: the Yuba River and the Feather River.

Poke 1: Yuba River

The only placer palladium deposits in the western Sierra Nevada foothills are found in the Yuba River (Figure 47), though other platinum group metals were known from other localities. Gold associated with these deposits is in the North San Juan Mining District in Nevada County (where gold grains are more angular) and in the Hammonton Mining District in Yuba County (where gold grains are more rounded).

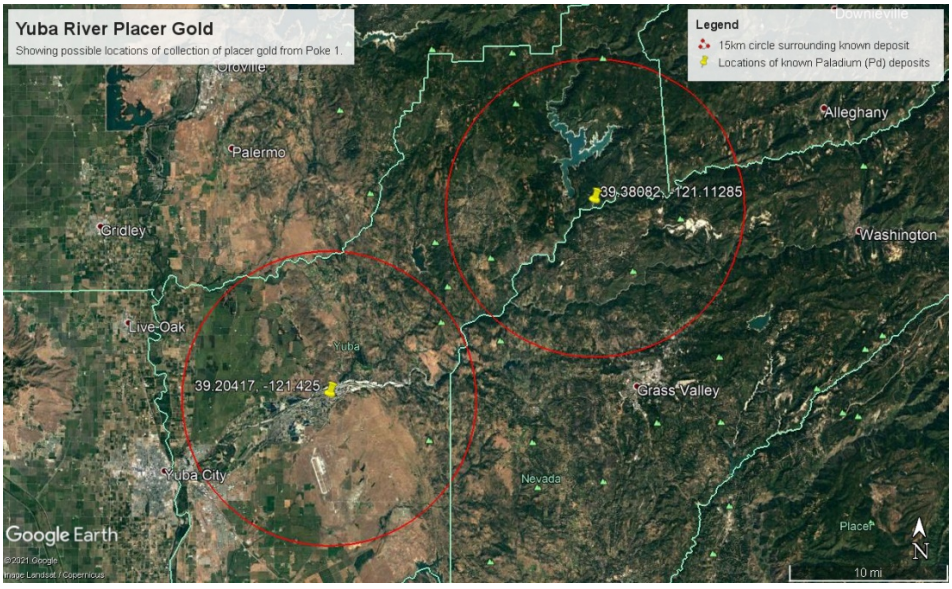

Figure 47. Showing possible locations along the Yuba River where placer gold from Poke 1 could have been collected from.

Poke 2: Upper Feather River

The presence of anglesite minerals in the form of inclusions tells us that they formed with the gold and can be used to fingerprint the deposit. The only deposits of anglesite associated with gold in the western Sierras are from Plumas County along the upper Feather River in the Granite Basin Mining District and the Last Chance Mining District (Figure 48).

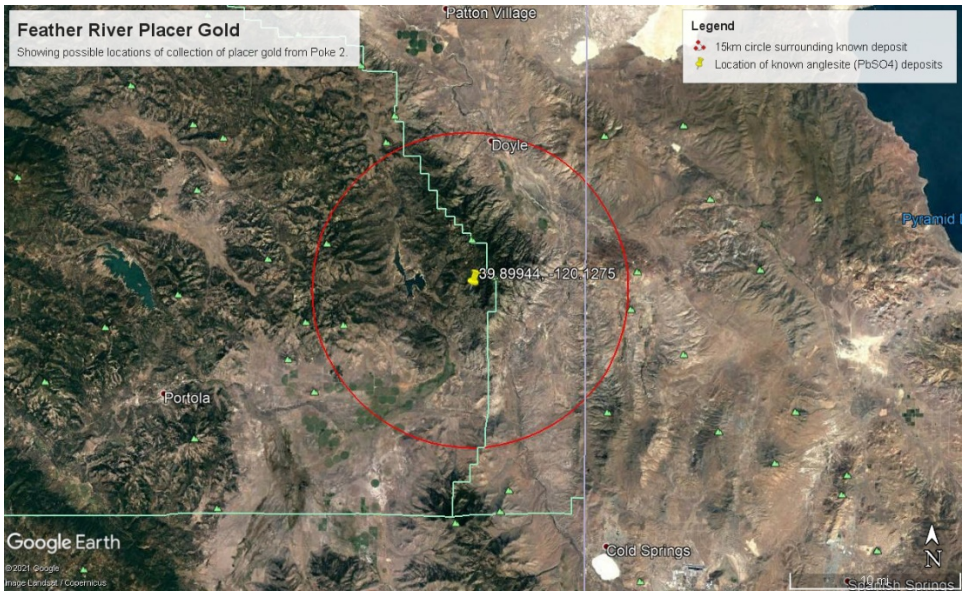

Figure 48. Showing possible locations along the Feather River where placer gold from Poke 2 could have been collected form.

Poke 3

Future work will need to be conducted to determine where in the Mother Lode region of California gold from Poke 3 was collected from.

Possible Owners

Gold Buyer

Most gold buyers who worked in California gold fields earned a living by serving as the middle-man between the miners who needed to stay at their mines and the assay offices that produced ingot in larger towns. They would often mix placer gold from different localities with known purities, to produce mixtures with a purity that was advantageous to specific refining techniques. But these gold buyers did not typically travel back East, and are unlikely to have traveled with raw placer gold. Rather, they would have converted their gold into an assayer's ingot with stamped values, that could be readily deposited at any bank in the nation. Furthermore, the particle sizes of the gold ranges so widely it is unlikely that an East Coast gold buyer was responsible for the transportation of the vest. These gold buyers were often employed by jewelers looking for specific pieces that can be used to make particular jewelry (ex: two complementing nuggets to make earrings, one large specimen piece for a brooch or necklace, etc.).

It is possible that the gold buyer requested to have a special run without the use of Hg. However, this seems highly unlikely as it would have caused the operation to "lose money." It is also possible that a gold buyer may have intended to sieve the gold upon arrival back at their office; however, this seems unlikely as it would have been transported in a more traditional shipping manner.

The presence of "black sands" further suggests the owner was not a gold buyer as they would have only been interested in the gold and not the dirt. It is

also unlikely that these were samples from or destined for a traveling academic, as few would have been able to afford kilogram-scale parcels of gold.

Individual Prospector

It is highly likely that an individual prospector or small partnership recovered the placer gold. Smaller operations could not afford the high cost of Hg and are more willing to lose the flour gold during their recovery operations.

The presence of the black sands in the pokes further suggests an individual owner that was transporting their private property as they wouldn’t have worried about refining or cleaning the gold in any specific way before storage.

Poke 2: “L. Darcey” or “J. Darcey”

Figure 49. Showing Poke 2 (#691-2) with the name “L. Darcey” or “J. Darcey” written along its side.

Upon returning to the Bob’s lab for placer gold samples from Poke 2 and Poke 3, it was discovered that a name was written along the side of Poke 2 (Figure 49). This created more questions than answer for me. The three main hypothesis I had for this was: (1) this was a recycled bag that was “borrowed” from Darcey, (2) the poke was meant to go to a Darcey upon returned to the Port of NY, and (3) this poke was sent on consignment, absent its owners (Darcey). The ”Darcey” name printed on the poke is preceded by a letter that looks initially

like the letter “L”. However, cursive writing of that time can be confusing to today’s reader, and there were many abbreviations used in the mid-1800s that are not used today.

I performed a check through online genealogy databases looking for an “L. Darcey.” Information was scarce. One possible match: a young man that immigrated from Liverpool, England to New York in the 1840s and would have been in his early 30s at the time of the sinking of the SS Central America. Future research will be needed to identify “L. Darcey”.

Another search for a “J. Darcey” yielded more promising results (Figures 50a and 50b). A census record from 1860 revealed that 24-year-old, Irish-born, J. Darcey lived in Upper Indian Creek, Del Norte, California. It is possible that young Mr. Darcey worked for a gold buyer and Poke 2 was the gold that he had collected for his employer. While this is not conclusive proof of ownership, it is a possibility that this poke once belonged to this individual, or a relative who was actually “L. Darcey,” or was shipped to that relative back East. Future genealogical work will be required to explore these possibilities.

Figure 50a. Showing results for “J. Darcey” from Del Norte, California in 1860.

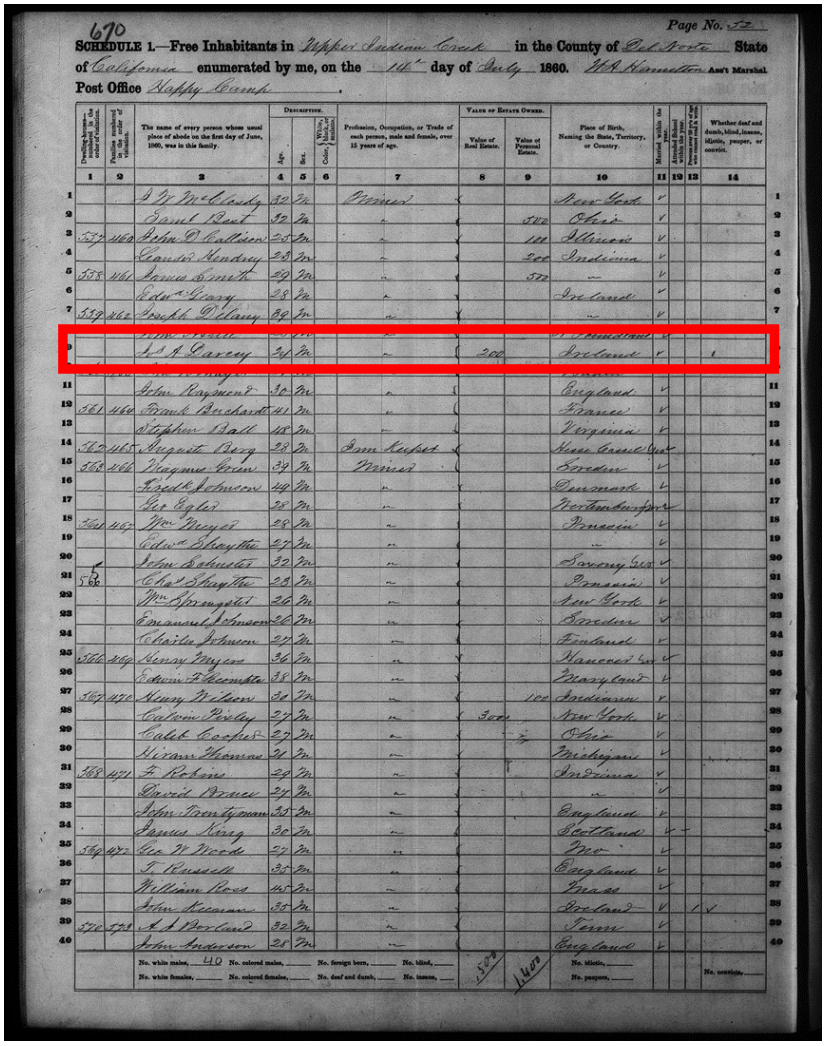

Figure 50b. Showing the census record from 1860 where J. Darcey's name appears (in red). Darcey resided in Upper Indian Creek in Del Norte, California with two other individuals.

CHAPTER EIGHT:

CONCLUSION

The finding of the SS Central America and its artifacts gives us an amazing glimpse into the lives of mid-19th century people that were aboard at the time of it sinking. The placer gold recovered from the ship's purser safe gives us further insight into the locations within the Mother Lode of California that prospectors were searching for gold. Geochemical analyses of placer gold, their inclusions, and accessory minerals from Poke 1 and Poke 2 point to the Yuba and Feather rivers, respectively. Future work will need to be done to determine the origin of gold from Poke 3. Traces of mercury on the surface of the gold suggests the mercury had anthropogenic origins and collection of the gold downstream from a significant mining operation. Finally, the finding of the gold in the ship's purser safe and not in the belongings of passengers or crew suggests this gold was gathered by a professional gold buyer or mining engineer with connections and discretion beyond those of a simple miner.

APPENDIX A:

GOLD DISTRICTS OF CALIFORNIA

Table 3a. Gold purity data from Amador county.

Amador County		
Name	*Purity*	
	Low	High
Buena Vista	880	940
Butte Flat	880	920
Clinton	860	880
Drytown	860	880
French Hill	920	930
Humbug	920	930
Irishtown	860	880
Jackson Creek	860	880
Lancha Plana	880	940
Mokelumne River	860	870
Red Hill	920	930
Slabtown	860	880
Sutter Creek	840	860
Stone Creek	850	
Tunnel Hill	920	
Willow Spring	860	
Brown's Flat	920	925
Douglasville	930	935
East Columbia	905	935
East Columbia (lower)	937	
East Columbia (upper)	920	
Knapp's Ranch	940	950
Matelot Gulch	930	
Pine Log	890	895
Ransomville	945	
Rio Vista	925	
San Diego Gulch	940	
Sawmill Flat	920	
Springfield Flat	920	
Three Pine	935	
Under lava beds at Gold Hill	968	
Yankee Hill	917	930
	Average	905
	Min	840
	Max	968
Source Data: Clark (1970), Hanks (1884), Lindgren (1911)		

Table 3b. Gold purity data of Butte County.

Butte County		
Name	*Purity*	
	Low	High
Blue Lead	950	
Butte Creek	880	
Bangor	910	
Cherokee	970	
Dogtown	880	
Dry Creek	925	
French Creek	870	
Forbestown	870	880
Forbes Ravine	898	
Hansonville	925	
Holt's Ravine	935	
Honcut	910	925
Kimshaw	920	
Main Feather River	890	900
Middle Fork Feather River	890	
Morris Ravine	918	920
Mooreville	890	
Nimshew	900	
North Fork Feather River	880	
Oregon House	900	
Ophir Flat	875	
Oroville	920	
Prairie House	925	
Rancheria	920	
South Fork Feather River	892	
Thompson's Flat	940	
Walker's Plain	920	
Willow Creek	900	
Wyandotte	900	
Yankee Flat	930	950
	Average	909
	Min	870
	Max	970
Source Data: Clark (1970), Hanks (1884), Lindgren (1911)		

Table 3c. Gold purity data of Calaveras County.

Calaveras County		
Name	*Purity*	
	Low	High
Albany	890	
Average	900	
Balaklava Hill	900	910
Byrne's Ferry	860	
Calaveras River	895	
Campo Seco	845	
Cave City	900	
Chile Gulch	890	
Central Hill	780	785
Chichi	935	935
Corral Flat	910	
Corral Hill	955	
Douglas Flat	900	
El Dorado	880	895
Empire Gulch	870	
French Gulch	870	875
Gravel Ridge	908	
Humbug Hill	928	947
Indian Creek	870	880
Jackson	935	945
Mokelumne Hill	930	
Murphy's	888	
Old Channel	905	
Old Gulch	895	
O'Neil's Creek	911	
Pennsylvania Gulch	908	
Owlbarron Flat	900	
Red Hill	840	850
Rich Gulch	895	
Salt Spring Valley	700	
San Andreas	900	
San Antonio	850	884
San Domingo	852	
Snake Gulch	875	880
Tunnel Hill	883	
Texas Gulch	895	
Union Claim	942	
Vallecito	900	945

Vallecito Hill	940	
Vallecito Flat	900	910
Waite's Flat	940	
Wm. Holmes	900	
	Average	891
	Min	700
	Max	955
Source Data: Clark (1970), Hanks (1884), Lindgren (1911)		

Table 3d. Gold purity of El Dorado County.

El Dorado County		
Name	*Purity*	
	Low	High
Aurum City	870	
Bottle Hill	888	
Brownsville	800	960
Buckeye Hill	910	
Buckeye Flat	850	
Big Cañon	857	
Cañon Creek	885	
Carson Creek	910	
Centerville	927	
Coloma	880	
Cosumnes	810	880
Clay Hill	915	
Coon Hill	965	
Coon Hollow	910	970
Cedarville and Mount Auburn	800	
Deer Creek	895	
Divide, between American and Weber Creek	850	900
Dogtown	825	
Dross Ravine	850	
Dry Creek	850	
Empire Ravine	885	
Empire Cañon	860	890
Fairplay	800	
French Creek	820	
French Town	840	

Georgetown	860	885
Gold Hill	890	900
Grizzly Flat	650	865
Green Valley	900	
Grizzly Gulch	850	
Hangtown Creek	900	
Hermitage Ranch	950	
Illinois Cañon	890	
Immigrant Ravine	910	
Indian Diggings	900	925
Indian Creek	890	
Indian Hill	950	
Johntown	885	
Kelsey	870	
Kentucky Hill	890	
Latrobe	890	
Matthews' Creek	890	
Manhattan Creek	940	
Missouri Flat	938	
Missouri Cañon	775	880
Mount Gregory	830	
New York Ravine	915	
Otter Creek	830	880
Oregon Cañon	890	
Pleasant Valley	910	
Newtown	910	
Plunkett's Ravine	905	
Quartz Cañon	840	
Quartz Hill	870	
Reservoir Hill	910	940
Rich Bar	885	
Rock Creek	890	
Shingle Springs	852	
Smith's Flat	975	
Spanish Hill	900	987
Spanish Camp	855	
Spanish Dry Diggings	750	880
Spring Hill	875	
Stillwagen's	675	
South Fork of American River	875	900
Slate Creek	850	
Sugar Loaf	968	

Uniontown	880	
Webber Creek	888	890
White Rock Hill	965	
West Cañon	890	
	Average	880
	Min	650
	Max	987
Source Data: Clark (1970), Hanks (1884), Lindgren (1911)		

Table 3e. Gold purity data of Nevada County.

Nevada County		
Name	*Purity*	
	Low	High
Alpha	908	968
American Hill	875	905
Arkansas Cañon	936	
Bear River	870	900
Blue Tent	885	925
Beckville	848	
Birchville	942	
Borrjers Ranch	847	
Bourbon Hill	837	844
Brandy City	870	
Brush Creek	958	961
Brown's Hill	905	
Buckeye Hill	877	
Canada Hill	545	
Cedar Ravine	865	
Cement Hill	840	852
Chalk Bluff	960	976
Christmas Hill	980	
Cherokee	910	920
Columbia Hill	822	961
Colton Hill	890	964
Cooley Hill	964	
Coyote Hill	850	860
Crumbeck Ravine	866	
Deer Creek	949	955
Rough and Ready	875	880

Diamond Creek	845	906
Eagle Ravine	848	
Eureka	825	870
Fall Creek	878	880
French Garden	820	
French Corral	800	
Gold Hill	965	970
Gold Cañon	920	
Gold Flat	815	837
Gopher Hill	825	936
Greenhorn	865	870
Green Mountain	916	
Grizzly Cañon	810	
Hunt's Hill	812	935
Humbug	920	953
Hitchcock Ravine	925	
Illinois Ravine	861	
Jackass Flat	874	
Jefferson Flat	874	
Jefferson Hill	911	
Jones' Bar	884	
Kanaka Creek	875	880
Kansas Hill	836	
Kentucky Flat	870	
Lawson Flat	877	
Liberty Hill	895	908
Little York	892	960
Little Deer Creek	845	850
Lost Hill	885	890
Lost Ravine	870	903
Lowell Hill	904	
Long Hollow	834	
Manzanita Hill	820	830
Miles' Ravine	860	
Middle Yuba	880	
Missouri Bar	883	884
Mount Oro	872	
Moore's Flat	860	875
Montezuma Hill	865	
Mosquito Creek	790	800
Mud Flat	818	
Myers' Ravine	860	870

Native American Ravine	884	
Nevada City	815	840
Newtown	825	
North Yuba	890	
Omega	950	975
Orleans Flat	895	910
Oregon Hill	875	890
Osbourne Hill	841	
Peck's Ravine	828	833
Phelps' Hill	820	913
Pleasant Valley	898	904
Picayune Point	850	890
Quaker Hill	922	960
Randolph Flat	920	
Rattlesnake	810	
Red Dog	860	930
Relief Hill	931	
Remington Hill	920	
Rock Creek	869	870
Round Mountain	834	879
Rush Creek	840	850
Sailors' Flat	870	875
San Juan North	960	
Selby Hill	814	865
Selby Flat	840	845
South Yuba	870	875
Scott's Flat	922	940
Shady Creek	900	910
Slate Creek	814	
Snow Point	880	885
Steep Hallow	900	903
Sweetland	900	930
Scotchman's Creek	897	822
San Juan, Columbia Hill, and Humbug	912	935
Timbuctoo	940	950
Thomas' Flat	854	
Ural	811	820
Virgin Flat	886	
Washington	870	886
Walloupa	852	910
Woods' Ravine	845	855

Wet Hill	855	875
Wolf Creek	825	910
Woolsey's Flat	910	
Wilcox Ravine	845	855
You Bet (blue gravel)	890	919
You Bet (red gravel)	907	984
Yankee Hill	917	
	Average	881
	Min	545
	Max	984
Source Data: Clark (1970), Hanks (1884), Lindgren (1911)		

Table 3f. Gold purity data of Placer County.

Placer County		
Name	*Purity*	
	Low	High
Antelope Ravine	770	
Antone	900	910
Auburn Ravine	810	
Bath	910	970
Bear River	900	930
Bear Valley	914	
Blue Gulch	925	
Blue Lead	930	944
Bird's Flat	893	
Bird Valley	830	890
Brushy Cañon	925	
Burnt Flat	893	
Cañon Creek	950	
Canada Hill	900	910
Cedar Company	965	
Colfax Ravine	900	
Damascus	900	
Deadwood	930	945
Devil's Basin	945	
Doten's Bar	870	
Doty's Bar	750	
Doty's Ravine	750	
Dutch Ravine	810	

Dutch Flat	934	970
Durtch Flat Ravine	930	
El Dorado Cañon	870	935
Elizabethtown	860	
Forest Hill	880	890
Gold Run	950	975
Green Valley	920	
Grizzly Flat	905	
Humbug Cañon	890	894
Huyck Company	945	
Illinoistown	794	
Indiana Hill	925	
Iowa Hill	900	
Last Chance	915	920
Ladies' Cañon	750	870
Long Cañon	930	
Lost Camp	940	
Mad Cañon	870	
Michigan Bluff	940	970
Michigan Flat	925	970
Middle Fork of American River	870	910
Millertown	800	
Miller's Defeat	916	
Miners' Ravine	760	
Nary Red	916	935
Nevada Company	945	
North Fork of American River	870	910
North Ravine	790	
Ophir	740	
Paradise	830	840
Pine Flat	800	
Red Hill	960	970
Roach Hill	918	
Rock Creek	910	
Rich Flat	915	
Rock Spring	690	
Secret Cañon	960	965
Taylor Company	965	
Van Cliff	900	910
Virginiatown	775	
Yankee Jim	900	
	Average	893

	Min	690
	Max	975
Source Data: Clark (1970), Hanks (1884), Lindgren (1911)		

Table 3g. Gold purity data of Plumas County.

Plumas County		
Name	*Purity*	
	Low	High
Jamison	860	
Laporte	940	945
Onion Valley	900	
Poorman's Creek	860	880
	Average	898
	Min	860
	Max	945
Source Data: Clark (1970), Hanks (1884), Lindgren (1911)		

Table 3h. Gold purity data of Sierra County.

Sierra County		
Name	*Purity*	
	Low	High
Alleghany	900	
American Hill	935	950
Bald Mountain	915	956
Balsam Flat	880	
Cañon Creek	880	
Cedar Grove	930	
Chaparrel Hill	905	
Chipps' Flat	880	
City of Six	900	
Chandlerville	920	940
Cold Cañon	918	
Craycroft	880	
Deadwood	840	
Downieville	885	
Eureka	840	905

Excelsior	905	
Fir Cap (Fir Gap)	828	
Forest City	900	
French Ravine	800	
Gibsonville	900	936
Hepsidam	900	
Hopkins' Creek	915	
Howland Flat	900	919
Kanaka Creek	860	
Ladies' Cañon	884	
Middle Yuba	875	
Monte Cristo	905	
Minnesota	880	
Near Sierra Buttes	920	
Nebraska (blue lead)	935	
Nelson	887	906
Oregon Creek	830	
Poker Flat	890	
Pine Grove	920	
Potosi	912	919
Poorman	910	
Port Wine	935	
Ravines near Laporte	900	
Richmond Hill	910	
Rock Creek	900	
Sawpit Flat	910	
Slate Creek	880	900
Smith's Flat	825	
Spanish Ranch	945	
St. Louis	900	925
Sweet Oil Diggings	875	
Union Company	870	
Washington Hill	906	
Wet Ravine	825	
Whisky Diggings	905	
Young American Flat	800	820
	Average	894
	Min	800
	Max	956
Source Data: Clark (1970), Hanks (1884), Lindgren (1911)		

Table 3i. Gold purity data of Tuolumne County.

Tuolumne County		
Name	*Purity*	
	Low	High
American Camp	850	
Cooper's Flat	735	825
Columbia	930	950
Golden Rule	800	
Jamestown	890	900
Montezuma	900	
Poverty Hill	890	900
Shaw's Flat	927	930
Springfield	930	960
Sonora	878	
Somerville	780	
Sugar Pine	900	920
Rawhide Ranch	850	
	Average	882
	Min	735
	Max	960
Source Data: Clark (1970), Hanks (1884), Lindgren (1911)		

Table 3j. Gold purity data of Yuba County.

Yuba County		
Name	*Purity*	
	Low	High
Brownsville	890	
Mooney Flat	900	940
Ousely's Bar	950	
Parks' Bar	960	
Timbuctoo	960	962
	Average	933
	Min	890
	Max	962
Source Data: Clark (1970), Hanks (1884), Lindgren (1911)		

APPENDIX B:

MODERN COMPARITIVE DATA

Table 4a. Quantification of gold sample from Yuba River: Yuba 2 with a purity of 99.86%.

Atomic number	Element symbol	Element name	Concentration (ppm)	Concentration (%)
79	Au	Gold	1594217	91.468
47	Ag	Silver	1447.46	0.083
29	Cu	Copper	836.88	0.048
46	Pd	Palladium	281.98	0.016
80	Hg	Mercury	32563.73	1.868
30	Zn	Zinc	9611.52	0.551
74	W	Tungsten	14127.1	0.811
26	Fe	Iron	24699.2	1.417
23	V	Vanadium	19.8	0.001
21	Sc	Scandium	22.03	0.001
20	Ca	Calcium	569.43	0.033
19	K	Potassium	2013.28	0.116
16	S	Sulfur	60353.39	3.463
52	Te	Tellurium	149.13	0.009
51	Sb	Antimony	84.42	0.005
50	Sn	Tin	338.62	0.019
39	Y	Yttrium	105.76	0.006
14	Si	Silicon	393.66	0.019
13	Al	Aluminum	1091.22	0.063

Table 4b. Quantification of gold sample from Yuba River: Yuba 2 with a gold purity of 99.59%.

Atomic number	Element symbol	Element name	Concentration (ppm)	Concentration (%)
79	Au	Gold	497728.04	80.071
47	Ag	Silver	1516.22	0.244
29	Cu	Copper	542.66	0.087
46	Pd	Palladium	318.13	0.051
80	Hg	Mercury	34691.17	5.581
30	Zn	Zinc	623.84	0.100
74	W	Tungsten	802.17	0.129
26	Fe	Iron	2364.42	0.380
23	V	Vanadium	21.62	0.003
21	Sc	Scandium	28.74	0.005
20	Ca	Calcium	775.87	0.125
19	K	Potassium	2104.15	0.338
16	S	Sulfur	78221.71	12.584
52	Te	Tellurium	211.03	0.034
50	Sn	Tin	316.26	0.051
14	Si	Silicon	501.31	0.081
13	Al	Aluminum	843.69	0.136

Table 4c. Quantification of gold sample from Yuba River: Yuba 3 with a gold purity of 99.69%

Atomic number	Element symbol	Element name	Concentration (ppm)	Concentration (%)
79	Au	Gold	534789.31	73.851
47	Ag	Silver	1146.01	0.158
29	Cu	Copper	520.42	0.072
46	Pd	Palladium	272.81	0.038
80	Hg	Mercury	35782.88	4.941
30	Zn	Zinc	1780.81	0.246
26	Fe	Iron	2256.74	0.312
23	V	Vanadium	18.7	0.003
21	Sc	Scandium	23.95	0.003
20	Ca	Calcium	1379.42	0.190
19	K	Potassium	2180.74	0.301
16	S	Sulfur	141942.7	19.601
52	Te	Tellurium	176.49	0.024
50	Sn	Tin	241.87	0.033
39	Y	Yttrium	146.08	0.020
14	Si	Silicon	455.44	0.063
13	Al	Aluminum	1033.75	0.143

Table 4d. Quantification of gold sample from Feather River: Feather 1 with a gold purity of 94.09%

Atomic number	Element symbol	Element name	Concentration (ppm)	Concentration (%)
79	Au	Gold	500039.59	59.178
47	Ag	Silver	31197.53	3.692
29	Cu	Copper	189.34	0.022
82	Pb	Lead	291.35	0.034
38	Sr	Strontium	154.26	0.018
92	U	Uranium	926.7	0.110
80	Hg	Mercury	37744.29	4.467
26	Fe	Iron	1431.33	0.169
22	Ti	Titanium	183.63	0.022
21	Sc	Scandium	19.02	0.002
20	Ca	Calcium	1556.69	0.184
19	K	Potassium	1022.84	0.121
16	S	Sulfur	124122.53	14.689
50	Sn	Tin	1271.84	0.151
14	Si	Silicon	117019.46	13.849
13	Al	Aluminum	27809.35	3.291

Table 4e. Quantification of gold sample from Feather River: Feather 2 with a gold purity of 95.26%

Atomic number	Element symbol	Element name	Concentration (ppm)	Concentration (%)
79	Au	Gold	555378.59	71.390
47	Ag	Silver	27521.68	3.538
29	Cu	Copper	118.85	0.015
82	Pb	Lead	130.21	0.017
42	Mo	Molybdenum	86.41	0.011
92	U	Uranium	673.4	0.087
90	Th	Thorium	68.03	0.009
80	Hg	Mercury	33136.11	4.259
26	Fe	Iron	1229.48	0.158
22	Ti	Titanium	159.5	0.021
21	Sc	Scandium	20.58	0.003
20	Ca	Calcium	1858.86	0.239
19	K	Potassium	4908.01	0.631
16	S	Sulfur	114070.31	14.663
50	Sn	Tin	1596.22	0.205
48	Cd	Cadmium	43.2	0.006
14	Si	Silicon	19535.3	2.511
13	Al	Aluminum	17413.63	2.238

Table 4f. Quantification of gold sample from Feather River: Feather 3 with a gold purity of 93.186%

Atomic number	Element symbol	Element name	Concentration (ppm)	Concentration (%)
79	Au	Gold	495669.81	64.374
47	Ag	Silver	36038.61	4.680
29	Cu	Copper	211.23	0.027
82	Pb	Lead	175.71	0.023
90	Th	Thorium	88.34	0.011
80	Hg	Mercury	14618.82	1.899
26	Fe	Iron	1766.22	0.229
23	V	Vanadium	8.4	0.001
22	Ti	Titanium	137.15	0.018
21	Sc	Scandium	12.39	0.002
20	Ca	Calcium	3822.47	0.496
19	K	Potassium	17421.3	2.263
16	S	Sulfur	101917.66	13.236
50	Sn	Tin	755.49	0.098
14	Si	Silicon	67284.6	8.738
13	Al	Aluminum	30056.66	3.904

APPENDIX C:

GOLD PURITY DATA

Table 5a. Showing gold purity data of fine placer gold from Poke 1.

Poke 1 – Fines				
Sample ID	*Au*	*Ag*	*Cu(x10)*	*Purity*
F.4.rnd1	63.706	2.887	0.53	94.91
F.4.rnd2	57.426	2.704	0.35	94.95
F.4.rnd3	64.453	2.813	0.46	95.17
F.4.rnd4	60.497	4.672	0.72	91.82
F.4.cry1	58.054	11.223	0.59	83.09
F.4.cry2	56.711	8.778	0.66	85.73
F.4.cry3	58.677	5.797	1.46	88.99
F.4.cry4	60.384	4.337	2.52	89.80
F.4.cry5	15.729	1.118	3.44	77.53
F.2.4.rnd1	64.118	3.784	0.39	93.89
F.2.4.rnd2	63.004	2.126	0.38	96.17
F.2.4.rnd3	62.751	2.441	0.33	95.77
F.2.4.rnd4	63.013	5.219	0.33	91.91
F.2.4.rnd5	60.935	5.206	0.41	91.56
F.2.4.rnd6	61.874	2.518	0.41	95.48
F.2.4.rnd7	61.115	3.838	0.31	93.64
F.2.4.rnd8	60.658	3.324	0.46	94.13
F.2.4.rnd9	62.608	3.603	0.46	93.91
F.2.4.rnd10	64.029	4.477	0.46	92.84
F.2.4.cry1	51.814	8.051	0.37	86.02
F.2.4.cry2	56.214	8.547	0.82	85.72
F.2.4.cry3	60.315	5.188	1.73	89.71
F.2.4.cry4	58.845	8.422	0.5	86.83
F.2.4.cry5	57.575	5.107	0.79	90.71
F.2.4.cry6	61.606	2.052	4.1	90.92
F.2.4.cry6.5	57.114	0.621	8.65	86.03
F.2.4.cry7	49.108	9.931	0.1	83.04
F.2.4.cry8	48.764	5.453	2.2	86.43
F.2.4.cry9	23.044	0.878	12.76	62.82
F.9.1	99.57	0	4.3	95.86
F.9.2	99.59	0	4.1	96.05
F.9.3.	100	0	0	99.99
F.10.2	96.59	3.02	3.9	93.31
Grp1.3/4.1	99.85	0	1.5	98.52
Grp1.3/4.2	94.36	0	2.9	97.02
Grp1.3/4.3	91.88	8.12	0	91.88
Grp1.6.1	87.74	0	1.3	98.54
Grp1.6.2	81.15	0	4.2	95.08
Grp1.6.3	99.64	0	3.6	96.51

Grp1.10.1	86.37	0	2	97.74
Grp1.10.2	89.84	0	0	89.87
Grp1.10.3	88.85	0	0	88.85
Pol.2.1	75.22	24.47	3.1	73.18
Pol.2.3	99.72	0	2.8	97.27
Pol.4.1	80.85	19.15	0	80.85
Pol.4.2	81.03	18.97	0	81.03
Pol.5.1	86.57	12.24	11.8	78.27
Pol.5.2	94.75	5.25	0	94.75
			Average	90.29
			Min	62.82
			Max	99.99

Table 5b. Showing gold purity data of ultrafine placer gold from Poke 1.

Poke 1 - Ultrafines				
Sample ID	*Au*	*Ag*	*Cu(x10)*	*Purity*
UofA.2uf	83.615	0.548	0	99.35
UofA.3uf	87.195	0.39	1.19	98.22
UofA.4uf	95.123	0.187	0.27	99.52
UofA.14uf	95.962	1.064	0.38	98.52
UofA.15uf	79.868	16.488	0	82.89
			Average	95.70
			Min	82.89
			Max	99.52

Table 5c. Showing gold purity data of the cores of placer gold recovered from Poke 1.

Poke 1 - Cores				
Sample ID	*Au*	*Ag*	*Cu(x10)*	*Purity*
Ssca1.6.4	78.82	21.18	0	78.82
Ssca1.12.4	83.48	16.52	0	83.48
B1.8.2	99.71	0	2.9	97.17
B1w.1.3	82.42	17.58	0	82.42
B1w.3.3	99.45	0	5.5	94.76
B1w.4.2	80.31	19.69	0	80.31
B1w.8.2	92.95	7.05	0	92.95
B1w.10.3	84.85	15.15	0	84.85
B1w.12.2	99.3	0.37	3.3	96.44
B1w.12.3	99.03	0.42	5.5	94.36
B1w.13.2	90.18	9.58	2.4	88.27
B1w.14.4	90.79	9.03	1.8	89.34
B1p2.4.3	77.47	0	2.6	96.75
B1p1.4.4	82.47	0	0	82.47
B1p2.8.2	84.02	15.98	0	84.02
UofA.4	79.6314	25.2771	0.206	75.76
UofA.5	78.701	25.5153	0.11	75.44
UofA.6	85.806	17.568	0.117	82.91
UofA.9	83.9614	17.0486	0.414	82.78
			Average	86.49
			Min	75.44
			Max	86.49

Table 5d. Showing gold purity data of the rims of placer gold recovered from Poke 1.

Poke 1 - Rims				
Sample ID	*Au*	*Ag*	*Cu(x10)*	*Purity*
Ssca1.6.3	99.58	0	0.42	99.58
Ssca1.12.3	84.88	15.12	0	84.88
B1w.1.1	95.03	0	0	95.03
B1w.1.2	99.26	0	7.4	93.06
B1w.4.1	99.76	0	2.4	97.65
B1w.8.1	99.47	0	5.3	94.94
B1w.10.2	85.66	14.34	0	85.66
B1w.12.1	99.61	0	3.9	96.23
B1w.13.1	99.57	0	4.3	95.86
B1w.14.3	99.57	0	4.3	95.86
B1p2.8.1	99.82	0	1.8	98.23
UofA.1	90.1615	1.5391	0	98.32
UofA.2	98.0231	4.0706	0.533	95.51
UofA.3	99.8382	2.4788	0	97.58
UofA.7	101.3373	1.1308	0.287	98.62
UofA.8	101.315	1.1714	0.587	98.29
			Average	95.33
			Min	84.88
			Max	99.58

Table 6a. Showing gold purity data of placer gold from Poke 2, fines.

Poke 2 – Fines				
Sample ID	*Au*	*Ag*	*Cu(x10)*	*Purity*
F.1.1	77.27	0.97	1.8	96.54
F.1.2	74.37	2.7	0	96.50
F.1.3	76.87	1.33	0	98.30
F.3.1	84.8	0	2.5	97.14
F.3.2	99.37	0	6.3	94.04
F.3.3	76.67	0	2.1	97.33
F.4.1	71.21	1.78	0	97.56
F.4.2	76.94	0	4.5	94.47
F.5.1	76.39	0.32	3.4	95.36
F.5.2	78.93	0.42	1.9	97.14
F.5.3	79.96	0	0	79.96
			Average	94.94

			Min	79.96
			Max	98.30

Table 6b. Showing gold purity data of placer gold from Poke 2, ultrafines.

Poke 2 - Ultrafines				
Sample ID	*Au*	*Ag*	*Cu(x10)*	*Purity*
UofA.5uf	79.175	5.57	0.79	92.56
UofA.6uf	99.431	0.223	1.46	98.34
UofA.7uf	84.686	0.207	0.69	98.95
UofA.8uf	82.153	0.362	0.7	98.72
UofA.9uf	91.546	0.365	1.33	98.18
UofA.10uf	60.863	0.106	1.94	96.75
UofA.11uf	91.581	0..98	0.7	98.82
UofA.12uf	93.96	0.098	0.4	99.47
			Average	97.72
			Min	92.56
			Max	99.47

Table 6c. Showing gold purity data of the cores of placer gold recovered from Poke 2.

Poke 2 - Cores				
Sample ID	*Au*	*Ag*	*Cu(x10)*	*Purity*
Pol.1.3	92.54	7.46	0	92.54
Pol.1.4	87.16	12.84	0	87.16
Pol.5.2	86.59	12.99	4.2	83.44
Pol.6.1	89.64	10.36	0	89.64
B2.2.3	94.72	5.28	0	94.72
B2.3.3	97.74	2.26	0	97.74
B2.3.6	94.94	4.85	2	93.27
B2.4.2	91.23	8.77	0	91.23
B2.4.3	93.55	6.25	1.9	91.99
B2.5.4	92.49	7.51	0	92.49
			Average	91.49
			Min	83.44
			Max	97.74

Table 6d. Showing gold purity data of the rims of placer gold recovered from Poke 2.

Poke 2 - Rims				
Sample ID	*Au*	*Ag*	*Cu(x10)*	*Purity*
Pol.1.1	82.72	2.32	0	97.27
Pol.5.1	98.42	1.58	0	98.42
B2.2.4	97.54	0	6.4	93.84
B2.3.7	99.72	0	2.8	97.27
B2.4.1	99.31	0.69	0	99.31
B2.4.4	99.81	0	1.9	98.13
B2.5.3	89.56	10.28	1.5	88.38
			Average	96.06
			Min	88.38
			Max	99.31

Table 7a. Showing gold purity data of the cores of placer gold recovered from Poke 3.

Poke 3 - Cores				
Sample ID	*Au*	*Ag*	*Cu(x10)*	*Purity*
B3.2.6	99.52	0	4.8	95.40
B3.3.4	93.75	6.25	0	93.75
B3.3.5	93.82	5.93	2.5	91.76
B3.7.3	77.34	22.37	2.9	75.37
B3.8.3	90.16	9.84	0	90.16
B3.8.7	89.9	10.1	0	89.9
B3.11.1	99.8	0	2	98.04
B3.11.3	78.79	13.88	2.3	82.96
B3.11.4	90.04	9.48	4.7	86.39
B3.18.2	95.07	4.93	0	95.07
B3.18.3	94.55	5.45	0	94.55
B3.19.2	99.62	0	3.8	96.33
UofA.11	91.6617	11.6179	0	88.75
UofA.12	92.4592	10.7079	0	89.62
UofA.14	94.3998	8.2725	0.233	91.73
UofA.11uf	91.6617	11.6179	0	88.75

UofA.12uf	92.4592	10.7079	0	89.62
UofA.14uf	94.3998	8.2725	0.233	91.73
			Average	90.65
			Min	75.37
			Max	98.04

Table 7b. Showing gold purity data of the rims of placer gold recovered from Poke 3.

Poke 3 – Rims				
Sample ID	*Au*	*Ag*	*Cu(x10)*	*Purity*
B3.3.3	96.19	3.21	5.9	91.35
B3.3.6	91.08	8.92	0	91.08
B3.7.2	82.55	17.25	2	81.09
B3.8.5	92.67	0.25	0	99.73
B3.18.1	99.49	0	5.1	98.12
B3.19.1	99.48	0	5.2	95.03
UofA.10	102.4552	0.4233	0.173	99.42
UofA.13	100.8132	0.5343	0	99.47
UofA.15	101.2519	0.863	0	99.15
UofA.10uf	102.4552	0.4233	0.173	99.42
UofA.13uf	100.8132	0.5343	0	99.47
UofA.15uf	101.2519	0.863	0	99.15
			Average	94.61
			Min	81.09
			Max	99.73

APPENDIX D:

INCLUSION DATA

Table 8a. Showing geochemical data of inclusions from Poke 1, fines.

Element Name	Element Symbol	Atomic Number	Poke 1 - Fines	
			F.10.1	*Pol.2.4*
Oxygen	O	8	15.61	
Iron	Fe	26	7.34	
Copper	Cu	29		0.9
Strontium	Sr	38	2.58	
Molybdenum	Mo	42	33.06	
Silver	Ag	47	1.76	
Iridium	Ir	77		99.1
Gold	Au	79	2.07	
Lead	Pb	62	37.58	

Table 8b. Showing geochemical data of inclusions from Poke 1, cores.

Element Name	Element Symbol	Atomic Number	Poke 1 - Cores				
			Ssca1.5	*Ssca1.6.1*	*Ssca1.6.2*	*Ssca1.12.1*	*Ssca1.12.2*
Carbon	C	6	8.58			10.83	7.83
Nitrogen	N	7					3.64
Oxygen	O	8	52.88	44.15	45.94		39
Magnesium	Mg	12	7.32	3.58			
Aluminum	Al	13	10.86	11.11			
Silicon	Si	14	17.08	15.91	17.3		
Sulfur	S	16	3.28			34.8	24.61
Potassium	K	19		2.3			
Iron	Fe	26		5.71	9.71	23.77	24.93
Nickel	Ni	28				30.6	
Copper	Cu	29			0.15		
Selenium	Se	34		1.27			
Molybdenum	Mo	42		8.07			
Silver	Ag	47		2.87	3.14		
Gold	Au	79		2.24	12.6		
			Uf.a1.1	*Uf.a1.2*	*Uf.a1.3*	*Uf.a1.4*	
Carbon	C	6	0.28	1.22	0.36	2.97	
Oxygen	O	8	3.55	2.75		41.95	
Magnesium	Mg	12		3.99			

Silicon	Si	14		5.44		5.66	
Sulfur	S	14				12.01	
Chlorine	Cl	17			16.14		
Calcium	Ca	20		12.47			
Iron	Fe	26		17.98			
Copper	Cu	29	0.18	0.78	0.35	0.62	
Silver	Ag	47	0.25				
Gold	Au	79	5.03		2.23	2.68	
Lead	Pb	62	90.72	35.37	80.93		
			B1w.3.1	*B1w.3.2*	*B1w.3.4*	*B1w.4.3*	*B1w.7.2*
Oxygen	O	8	56.63	59.68	53.1	50.53	59.68
Sodium	Na	11				11.33	
Aluminum	Al	13	21.32	4.42	20.4	10.93	
Silicon	Si	14	22.05	1.75	20	25.2	36.91
Titanium	Ti	22		26.21			
Iron	Fe	26		3.78	6.5		
Zirconium	Zr	40		0.93			
Molybdenum	Mo	42		2.03			
Tin	Sn	50					1.88
Barium	Ba	56					1.53
Gold	Au	79				2	
			B1w.8.3	*B1w.13.3*	*B1w.14.1*	*B1w.14.2*	
Oxygen	O	8	54.03				
Magnesium	Mg	12	10.17				
Aluminum	Al	13	11.82				
Silicon	Si	14	13	87.29	88.49	87.34	
Iron	Fe	26	10.97				
Tin	Sn	50		12.71	11.51	12.66	
			B1w.14.5	*B1w.15.1*	*B1p2.4.2*		
Carbon	C	6	37.14		2.74		
Oxygen	O	8	62.86	52.03			
Magnesium	Mg	12		8.8			
Aluminum	Al	13		3.51			
Silicon	Si	14		20.11			
Sulfur	S	16			12.85		
Calcium	Ca	20		6.2			
Iron	Fe	26		9.35	24.6		
Lead	Pb	62			59.74		

Table 9. Showing geochemical data of inclusions from Poke 2.

Element Name	Element Symbol	Atomic Number	Poke 2				
			B2.2.1	*B2.2.2*	*B2.2.2*	*B2.3.1*	*B2.3.2*
Oxygen	O	8				20.08	37.33
Aluminum	Al	13					1.48
Silicon	Si	14					1.95
Sulfur	S	16	37.79	37.16	38.14	12.88	
Iron	Fe	26	36.32	29.44	37.32		44.15
Copper	Cu	29	25.9	33.4	24.53		
Lead	Pb	62				67.04	15.09
			B2.3.4	*B2.3.5*	*B2.5.1*	*B2.5.2*	
Oxygen	O	8	20.58	22.69	42.88	44.32	
Sodium	Na	11				12.88	
Magnesium	Mg	12			1.54		
Aluminum	Al	13			10.08	11.33	
Silicon	Si	14			23.82	31.47	
Sulfur	S	16	12.46	12.39	2.52		
Titanium	Ti	22			0.94		
Iron	Fe	26			18.21		
Lead	Pb	62	66.95	64.93			

Table 10. Showing geochemical data of inclusions from Poke 3.

Element Name	Element Symbol	Atomic Number	Poke 3				
			B3.2.1	*B3.2.2*	*B3.2.3*	*B3.3.1*	*B3.3.2*
Oxygen	O	8	42.51	43.56	2.68	44.02	51.93
Magnesium	Mg	12	2.88				
Aluminum	Al	13	13.16	14.5		14.752	
Silicon	Si	14	23.81	29.02	91.74	21.85	48.07
Iron	Fe	26	5.67	8.75		17.44	
Copper	Cu	29	0.32		0.29		
Zirconium	Zr	40	3.6				
Niobium	Nb	41	7.31				
Silver	Ag	47	0.75	0.81		0.7	
Gold	Au	79		3.36	5.29	1.27	
			B3.7.1	*B3.8.1*	*B3.8.2*	*B3.8.6*	
Oxygen	O	8	41.89	42.99	44.03		
Sodium	Na	11		13.7			
Magnesium	Mg	12	7.27				
Aluminum	Al	13	11.91	11.4	13.57		
Silicon	Si	14	24.93	31.91	23.87		
Sulfur	S	16				56.67	
Iron	Fe	26	13.99		18.52	43.33	
			B3.10	*B3.12.1*	*B3.12.2*		
Sulfur	S	16	56.68	56.6	56.56		
Iron	Fe	26	43.32	43.4	43.44		

APPENDIX E:

ACCESSORY MINERAL DATA

Table 11a. Geochemical data of accessory minerals from Poke 1.

Element Name	Element Symbol	Atomic Number	Poke 1				
			f.24m	*f.2.4s*	*f.7*	*Uf.b1.1*	*Uf.b1.2*
Carbon	C	6				0.28	1.22
Oxygen	O	8			17.18	3.55	22.75
Magnesium	Mg	12					3.99
Silicon	Si	14	1.939		18.43		5.44
Phosphorous	P	15	5.712				
Sulfur	S	16	23.857	5.1			
Chlorine	Cl	17	0.272				
Potassium	K	19		0.197			
Calcium	Ca	20	0.369	0.084			12.47
Scandium	Sc	21		0.001			
Titanium	Ti	22		0.023			
Vanadium	V	23		0.002			
Chromium	Cr	24		0.025			
Manganese	Mn	25		0.128			3.99
Iron	Fe	26	5.738	14.12			17.98
Nickel	Ni	28	1.055	2.563			
Copper	Cu	29	0.396	0.846		0.18	0.78
Zinc	Zn	30	0.305	0.508			
Arsenic	As	33	5.278	4.915			
Yttrium	Y	39	0.11				
Zirconium	Zr	40		0.012	64.38		
Molybdenum	Mo	42		0.091			
Silver	Ag	47	2.926	1.085		0.25	
Tin	Sn	50		0.64			
Lead	Pb	62	9.56	15.264		90.72	35.37
Tungsten	W	74		0.343			
Gold	Au	79	42.267	53.95		5.03	
Mercury	Hg	80		0.678			
Bismuth	Bi	83	0.214				
			Uf.b2	*Uf.b3.1*	*B1.11*	*B1.12*	*B1w.7.1*
Carbon	C	6	0.37	2.61			
Oxygen	O	8	4.43	21.6	7.57	6.21	46.55
Silicon	Si	14	0.55	36.18			
Iron	Fe	26	39.39	13.19	92.43	93.79	28.19
Zirconium	Zr	40		7.35			

Niobium	Nb	41		19.07			
			B1w.7.2	*B1w.9.1*	*B1w.9.2*	*B1w.9.3*	*B1w.9.4*
Oxygen	O	8	59.68	39.54	42.33	5.61	44.85
Silicon	Si	14	36.91		14.32	0.94	13.71
Iron	Fe	26		60.46		10.29	
Copper	Cu	29				54.14	
Zirconium	Zr	40			43.35	2.32	41.43
Niobium	Nb	41				1.57	
			B1w.9.5	*B1w.10.1*	*B1p2.1.1*	*B1p2.1.3*	*B1p2.6.1*
Carbon	C	6				4.87	3.7
Oxygen	O	8	45.86	6.04	46.01	39.33	35.68
Silicon	Si	14			16.77		15.58
Sulfur	S	16		26.51			
Calcium	Ca	20			18.06		21.17
Titanium	Ti	22	25.22		19.17	25.83	23.87
Iron	Fe	26	28.92	11.3		29.97	
Copper	Cu	29		55.86			
			B1p2.6.2	*B1p2.6.3*	*UofA.pd*	*UofA.py*	
Carbon	C	6	3.42	2.78			
Oxygen	O	8	25.24	33.82			
Titanium	Ti	22	7.34	27.79			
Iron	Fe	26	64	35.61			
Copper	Cu	29				0.079	
Silver	Ag	47			13.612		
Osmium	Os	76				0.012	
Platinum	Pt	78			0.053		
Gold	Au	79				0.135	
Mercury	Hg	80			0.741	29.282	

Table 11b. Geochemical data of maps of accessory minerals from Poke 2.

Element Name	**Element Symbol**	**Atomic Number**	**Poke 1 - Maps**				
			B1p2.5	*B1p2.7*			
Carbon	C	6	19.94	3.96			
Silicon	Si	14	16.42	4.58			
Calcium	Ca	20	22.66	5.22			

Titanium	Ti	22	24.99	37.16			
Iron	Fe	26	11.08	49.08			
Gold	Au	79	4.9				

Table 11c. Geochemical data of line scan of accessory mineral from Poke 2.

Element Name	**Element Symbol**	**Atomic Number**	**Poke 1 – Line Scan**				
			B1p2.6				
Boron	B	5	3.45				
Carbon	C	6	2.31				
Oxygen	O	8	27.09				
Titanium	Ti	22	25.67				
Iron	Fe	26	41.48				

Table 12. Geochemical data of accessory minerals found in Poke 2.

Element Name	**Element Symbol**	**Atomic Number**	**Poke 2**				
			Uf.b2.1.1	*Uf.b2.1.2*	*Uf.b2.1.3*		
Oxygen	O	8	48	46.62	48.28		
Sodium	Na	11			12.69		
Magnesium	Mg	12	9.68	8.53			
Aluminum	Al	13		2.45	10.43		
Silicon	Si	14	23.92	24.55	28.6		
Calcium	Ca	20	6.91	6.54			
Iron	Fe	26	11.49	11.32			

APPENDIX F:

MORPHOLOGY DATA

Table 13a. Showing FI and distance data from placer gold nuggets recovered from Poke 1.

Poke 1 - nuggets							
	Length (mm)	**Width (mm)**	**Thickness (mm)**	**T/W**	**W/L**	**FI**	**Distance(km)**
4mm							
	1.6	0.483	0.064	0.13	0.30	16.3	75.9
	1.335	0.553	0.135	0.24	0.41	7.0	12.8
	1.197	0.677	0.15	0.22	0.57	6.2	10.1
	1.22	1.013	0.48	0.48	0.83	2.3	1.7
	1.132	0.752	0.33	0.44	0.66	2.9	2.2
	1.074	0.929	0.392	0.42	0.86	2.6	1.9
	0.737	0.692	0.323	0.47	0.94	2.2	1.6
	1.666	0.797	0.675	0.85	0.48	1.8	1.3
	0.916	0.726	0.68	0.94	0.79	1.2	1.0
2-4mm							
	1.438	0.543	0.15	0.28	0.38	6.6	11.3
	0.813	0.3	0.104	0.35	0.37	5.4	7.3
	1.019	0.551	0.1	0.18	0.54	7.9	16.3
	0.724	0.498	0.09	0.18	0.69	6.8	12.0
	0.655	0.411	0.08	0.19	0.63	6.7	11.5
	0.544	0.387	0.09	0.23	0.73	5.2	6.8
	0.657	0.39	0.07	0.18	0.59	7.5	14.7
	0.379	0.284	0.05	0.18	0.75	6.6	11.4
	0.322	0.266	0.03	0.11	0.83	9.8	26.1
	0.174	0.136	0.02	0.15	0.78	7.8	15.9
	0.8	0.344	0.264	0.77	0.43	2.2	1.5
	0.9	0.386	0.25	0.65	0.43	2.6	1.9
	1.006	0.479	0.25	0.52	0.48	3.0	2.4
	0.583	0.294	0.27	0.92	0.50	1.6	1.2
	0.502	0.275	0.16	0.58	0.55	2.4	1.8
	0.321	0.261	0.18	0.69	0.81	1.6	1.2
	0.352	0.21	0.1	0.48	0.60	2.8	2.2
	0.614	0.153	0.128	0.84	0.25	3.0	2.4

	0.572	0.203	0.16	0.79	0.35	2.4	1.7
	0.14	0.11	0.06	0.55	0.79	2.1	1.5

Table 13b. Showing FI and distance data from placer gold recovered from Poke 1, fines.

Poke 1 – fines							
	Length (µm)	**Width (µm)**	**Thickness (µm)**	**T/W**	**W/L**	**FI**	**Distance(km)**
F250grp1							
	450	210	50	0.24	0.47	6.6	11.3
	365	200	45	0.23	0.55	6.3	10.2
	490	270	52	0.19	0.55	7.3	14.0
	800	320	65	0.20	0.40	8.6	19.9
	1070	340	55	0.16	0.32	12.8	46.0
F250grp2							
	860	270	47	0.17	0.31	12.0	40.2
	520	320	58	0.18	0.62	7.2	13.7
	490	340	60	0.18	0.69	6.9	12.5

Table 14. Showing flatness index and distance date for the ultrafines of Poke 2.

Poke 2 – ultrafines							
	Length (µm)	**Width (µm)**	**Thickness (µm)**	**T/W**	**W/L**	**FI**	**Distance(km)**
	590	325	90	0.276923	0.550847	5.1	6.5
	750	300	125	0.416667	0.4	4.2	4.5
	580	275	110	0.4	0.474138	3.9	3.8
	390	250	120	0.48	0.641026	2.7	2.0
	475	210	105	0.5	0.442105	3.3	2.8
	1100	290	125	0.431034	0.263636	5.6	7.9
	1350	250	190	0.76	0.185185	4.2	4.5
	610	280	210	0.75	0.459016	2.1	1.5
	625	220	190	0.863636	0.352	2.2	1.6
	950	280	210	0.75	0.294737	2.9	2.3
	1160	200	190	0.95	0.172414	3.6	3.3
	780	100	100	1	0.128205	4.4	4.9

	615	75	65	0.866667	0.121951	5.3	7.2
	765	95	75	0.789474	0.124183	5.7	8.4
	605	280	190	0.678571	0.46281	2.3	1.7
	510	290	210	0.724138	0.568627	1.9	1.3
	675	270	195	0.722222	0.4	2.4	1.7

REFERENCES

911 Metallurgist, 2016, Types of Placers, https://www.911metallurgist.com/blog/list-types-placers, website, accessed February 2021.

Armstrong, J.T., 1988, Quantitative analysis of silicates and oxide minerals: Comparison of Monte-Carlo, ZAF and Phi-Rho-Z procedures, *in* Newbury, D.E., ed., Proceedings of the Microbeam Analysis Society: San Francisco, California, San Francisco Press, v. 23, p. 239-246.

Baumgart, D., 2009, Flumes Were Water Highways During the Gold Rush: Nevada County Gold, website, https://www.nevadacountygold.com/about/nevada-county-history/california-gold-rush-stories/flumes-were-water-highways-during-the-gold-rush, accessed Aug 2020.

Beesley, D., 2000, Beyond Gilbert: environmental history and hydraulic mining in the Sierra Nevada: The Mining History Journal, v. 7.

Blott, S.J. and Pye, K., 2008, Particle Shape: a review and new methods of characterization and classification, Sedimentology, v. 55, pgs. 31 – 63, doi: 10.1111/j.1365-3091.2007.00892.x.

Böhlke, J.R., 1999, California Gold: United States Geological Survey, Geological Society of America, Special Paper 338, doi: 10.1130/0-8137-2338-8.41.

Cailleux, A. and Tricart J., 1959, Introduction to the study of sand and pebbles: Cent. Doc. Univ. Paris, v. 3, 364 p., 194 p., and 202 p.

Clark, W. B., 1970, Gold Districts of California: California Division of Mines and Geology Bulletin 193, 186 p.

Coloma, 2020, The California Gold Rush of 1849, https://www.coloma.com/california-gold-discovery/history/california-gold-rush/, website, accessed February 2020.

Conrad, J., 1988, Story of an American Tragedy: Survivors' Accounts of the Sinking of the Steamship Central America: Columbus-America Group Press, 82 p.

Craw, D., Youngson, J. H., and Koons, P. O., 1999, Gold dispersal and placer formation in an active oblique collisional mountain belt, Southern Alps, New Zealand: Economic Geology, v. 94, p. 605-614.

Donovan, J.J., Snyder, D.A., and Rivers, M.L., 1993, An improved interference correction for trace element analysis: Microbeam Analysis, v. 2, p. 23–28.

Dunning, G., 1997, Tools of the Trade: Cobblestone, v. 18, issue 9, pg. 8.

Encyclopedia Britannica, 2020, California Gold Rush, https://www.britannica.com/biography/John-Sutter, website, accessed February 2020.

Evans, B, 2018, Personal Correspondence.

Fifty-second Congress, 1893, Session II, Ch. 183: US Code, Title 33, Chapter 14, https://www.law.cornell.edu/uscode/text/33/chapter-14, website, accessed Feb 2019.

Gilbert, G.K., 1917, Hydraulic-mining debris in the Sierra Nevada: USGS, Profession Paper 105, doi: 10.3133/pp105.

Hanks, H.G., 1884, Fourth Annual Report of the State Mineralogist for the Year Ending May 15, 1884: California State Mining Bureau, Sacramento, p. 219-224.

Harden, D.R., 2004, California Geology: Prentice Hall, New Jersey, 479 p.

Harper, J., 2012, California Gold Belts, https://www.mindat.org/photo-488262.html, website, accessed February 2021.

Helmenstine, T., 2018, Abundance of Elements in Earth's Crust – Periodic Table and List, https://sciencenotes.org/abundance-of-elements-in-earths-crust-periodic-table-and-list/, website, accessed April 2020.

Hérail, G., Fornari, M., Viscarra, G., and Miranda, V., 1990, Morphological and chemical evolution of gold grains during the formation of a polygenic fluviatile placer: the Mio-Pleistocene Tipuani placer example (Andes, Bolivia): Chronicle of Mining Research, v. 500, p. 41 - 49.

Herndon, W.L. and Gibbon, L., 1854, Exploration of the Valley of the Amazon: Grove Press, 256 p.

Herdendorf, C.E., 1995, Science on a deep-ocean shipwreck: Ohio Journal of Science, v. 95, no. 1, 212 p.

Kelley, R.L., 1954, Forgotten giant: the hydraulic gold mining industry in California: Pacific Historical Review, University of California Press, v. 23, no. 4, pp. 343-356.

Kelley, R.L., 1959, Gold vs. Grain, The Hydraulic Mining Controversy in California's Sacramento Valley, The Arthur H. Clark Company, Glendale, 327 p.

Kiester, Jr., E., 1999, Turning Water to Gold: Smithsonian, v. 30, no. 5.

Kinder, G., 1998, Ship of Gold in the Deep Blue Sea: Grove Press, 560 p.

Klare, N.E., 1992, The Final Voyage of the Central America, 1857: Klare-Taylor Publishing, 278 p.

Knight, J. B., Morison, S. R., and Mortensen, J. K., 1999, The relationship between placer gold particle shape, rimming, and distance of fluvial transport as exemplified by gold from the Klondike District, Yukon Territory, Canada: Economic Geology, v. 94, p. 635-648.

Landsea, C.W. and Franklin, J.L., 2013, HURDAT Atlantic Hurricane Database Uncertainty and Presentation of a New Database Format. Mon. Wea. Rev., 141, 3576-3592, website, https://www.nhc.noaa.gov/data/#tracks_all, accessed Aug 2020.

Lindgren, W., 1895, Characteristic features of California gold-quartz veins, Bulletin of the Geological Society of America, v. 6, pp. 221 – 240.

Lindgren, W. and Knowlton, F. H., 1911, The tertiary gravels of the Sierra Nevada of California: Professional Paper, v. 73, p. 226.

Maury, M.F., 1855, The Physical Geography of the Sea: Sampson, Low, Son & Co., https://doi.org/10.5962/bhl.title.102148.

Melchiorre, E.B., Kamenov, G.D., Sheets-Harris, C., Andronikov, A., Leatham, W.B., Yahn, J., and Lauretta, D.S., 2017, Climate-induced geochemical and morphological evolution of placer gold deposits at Rich Hill: GSA Bulletin, v. 129, p. 193–202, doi: 10.1130/B31522.1.

Melchiorre E.B., Seymour B.H. and Evans R.D. (2019). The interpretation of biogeochemical growths on gold coins from the SS Central America shipwreck: applications for biogeochemistry and geoarchaeology. *Journal of Marine Science and Engineering*, **7**, 209-225.

Mindat.org, 2020, Anglesite Locations, California, https://www.mindat.org/minlocsearch.php?frm_id=mls&cform_is_valid=1&cf_mls_page=1&minname=anglesite&region=california, website, accessed April 2020.

Mindat.org, 2020, Palladium Locations, California, https://www.mindat.org/minlocsearch.php?frm_id=mls&cform_is_valid=1&cf_mls_page=1&minname=palladium&region=california&sort=0&submit_mls=Search, website, accessed April 2020.

Museum of the City of San Francisco, 2020, California Gold Rush Chronology 1846-1849, http://www.sfmuseum.org/hist/chron1.html, website, accessed March 2020.

Oakland Museum of California, 1998, Gold Fever!, website, http://explore.museumca.org/goldrush/fever15.html, accessed Aug 2020.

Sandham, H., 2010, The Sluice: Wikimedia Commons, website, https://en.wikipedia.org/wiki/File:Henry_Sandham_-_The_Sluice.jpg, accessed Aug 2020.

Sandham, H., 2016, The Cradle: Wikimedia Commons, website, https://commons.wikimedia.org/wiki/File:Henry_Sandham_-_The_Cradle.jpg, accessed Aug 2020.

Sawyer Decision, Woodruff v. North Bloomfield Gravel Mining Co. and Others: Circuit Court D, California, January 7, 1884.

Schweichkert, R.A., Bogen, N.I., Girty, G.H., Hanson, R.E., and Mergeurian, C., 1984, Timing and structural expression of the Nevadan Orrogeny, Sierra Nevada, California: Geological Society of America Bulletin, v. 95, p. 967-979.

Seymour, B., 2018, The origin of biogenic growths on gold recovered from the SS Central America shipwreck: implications for geoarchaeology: California State University, San Bernardino, 30 p.

Shuster, J., Johnston, W.C., Magarvey, A.N., Gordon, A.R., Barron, K., Banerjee, R.N., and Southam, G., 2015, Structural and chemical characterization of placer gold grains: Implications for bacterial contributions to grain formation: Geomicrobiology Journal, v. 32, p. 158-169.

Sierra College, 2009, Mining Techniques of the Sierra Nevada and Gold Country: Journal of Sierra Nevada History & Biography, Sierra College Press, vol. 2, no. 1.

Silva, M., 1986, Placer Gold Recovery Methods: California Department of Conservation, Division of Mines and Geology, Special Publication 87, 37 p.

Sjoberg, J. and Gomes, J.M., 1981, Platinum-Group minerals in alluvial deposits northern and central California: California Geology, p. 91-103.

Thompson, T., 1998, America's Lost Treasure: A Pictorial Chronicle of the Sinking and Recovery of the United States Mail Steamship Central America: New York, The Atlantic Monthly Press, 191 p.

Turner, H.W., 1894, Notes on the gold ore of California: American Journal of Science (1880 – 1910); New Haven, v. 47, i. 282, 467 p.

USNA, 2020, Herndon Climb, website, https://www.usna.edu/PAO/faq_pages/herndon.php, accessed Aug 2020.

USS Constitution Museum, 2011, Sailor's Story: Purser Thomas Chew, website, https://ussconstitutionmuseum.org/discover-learn/educator-resources/?_sft_types=sailors-stories, accessed Aug 2020.

Wikipedia, 2019, George Law (financier), https://en.wikipedia.org/wiki/George_Law_(financier), website, accessed Jan 2020.

Wikipedia, 2020, William Lewis Herndon, https://en.wikipedia.org/wiki/William_Lewis_Herndon, website, accessed April 2020.

Wikipedia, 2020, US Mail Steamship Company, https://en.wikipedia.org/wiki/U.S._Mail_Steamship_Company, website, accessed Jan 2020.

Zingg, T., 1935, Contributions to the shadow analysis: Swiss Mineralogical and Petrological Communications, v. 15, p. 39-140.